

Identify As A Human Does: A Pathfinder of Next-Generation Anti-Cheat Framework for First-Person Shooter Games

Jiayi Zhang^{1,3}, Chenxin Sun^{1,3}, Yue Gu¹, Qingyu Zhang¹, Jiayi Lin¹, Xiaojiang Du^{2,4}, and Chenxiong Qian^{1,4}

¹*Department of Computer Science, University of Hong Kong, Hong Kong SAR*

²*Charles V. Schaefer, Jr. School of Engineering and Science, Stevens Institute of Technology, USA*

³Equal Contribution.

⁴Corresponding Authors.

Abstract

The gaming industry has experienced substantial growth, but cheating in online games poses a significant threat to the integrity of the gaming experience. Cheating, particularly in first-person shooter (FPS) games, can lead to substantial losses for the game industry. Existing anti-cheat solutions have limitations, such as client-side hardware constraints, security risks, server-side unreliable methods, and both-sides suffer from a lack of comprehensive real-world datasets. To address these limitations, the paper proposes HAWK, a server-side FPS anti-cheat framework for the popular game CS:GO. HAWK utilizes machine learning techniques to mimic human experts' identification process, leverages novel multi-view features, and it is equipped with a well-defined workflow. The authors evaluate HAWK with the first large and real-world datasets containing multiple cheat types and cheating sophistication, and it exhibits promising efficiency and acceptable overheads, shorter ban times compared to the in-use anti-cheat, a significant reduction in manual labor, and the ability to capture cheaters who evaded official inspections.

1 Introduction

The gaming industry has experienced substantial growth recently, with the global game market generating \$184.0 billion in 2023 and projected to reach \$218.7 billion in 2024 [47, 48]. However, cheating in online games poses a significant threat to the integrity of gaming experiences and disrupts game-play balance. In 2023 alone, cheating led to an estimated \$29 billion in losses, with 78% of gamers deterred from playing due to cheating [32]. In particular, first-person shooter (FPS) games, which account for 20.9% of total game sales and rank second among all genres [63], are particularly targeted by cheat developers seeking monetary gains due to their competitive and multiplayer nature. The most prevalent forms of cheating involve the use of *aimbots* to enhance a player's precision and *wallhacks* to reveal opponents' positions, thereby compromising game integrity [4, 9, 40].

On realizing the critical importance of game security [25], both academia and industry have proposed many anti-cheats solutions, applied either on the client-side [9, 49, 58] or server-side [2, 24, 27, 39, 69, 70]. However, current solutions have the following limitations.

Client-side solutions face hardware constraints, bring security and privacy concerns, or incur unacceptable system overheads. Two state-of-the-art systems [9, 49] require specific Trusted Execution Environments (TEEs) like Intel SGX. This dependence on particular hardware, which was deprecated in 2021 [5, 31], limits compatibility and practicality for industrial use. Some solutions involve scanning hard drives and gaining root privileges, posing risks of unauthorized access and personal data leakage [43, 45, 66]. Vulnerabilities, such as RCE exploits [8] and CVEs [15–18], demonstrate the potential for system instability and privacy breaches. The others rely on continuous surveillance or frequent patching to counter varying cheat signatures [3, 22, 35, 58], leading to increased client-side system overheads.

On the other hand, the existing server-side solutions use basic features and share low recall and accuracy. For instance, some solutions [2, 24, 27, 39, 69, 70] use features like winning rates or playtime, which are insufficient for detecting complex cheats such as *aimbots* or *wallhacks*. These methods also lack robust workflows to examine false positives, especially in noise-rich, real-world datasets. Additionally, they show low recall and accuracy in the real world, with extended ban cycles taking days or weeks [33, 50]. Incidents like the 2024 APEX Legends tournament hack [59] highlight the inefficacy of existing solutions under commercial anti-cheats such as Easy Anti-Cheat (EAC) [22].

Moreover, both client-side and server-side solutions suffer from a lack of comprehensive datasets, often relying on limited or synthetic data [2, 9, 24, 39, 49, 70], which may not represent real-world cheating scenarios. The simulated datasets lack varying levels of cheating sophistication (explained in Section 2.2), which could result in performance degradation or even failure in complex real-world scenarios.

To address the aforementioned limitations, we propose

HAWK, a server-side approach designed to analyze data transmitted to the server, thereby avoiding the inherent limitations of client-side solutions. HAWK introduces a comprehensive set of multi-view features and a robust framework to meticulously monitor players’ points of view, statistics, and behavioral consistencies. This approach includes a corresponding workflow aimed at shortening the ban cycle and considering the occurrence of false positives. HAWK achieves high detection recall and acceptable accuracy across large, real-world datasets with varying levels of cheating sophistication.

The key innovation of HAWK lies in its ability to mimic how human experts identify cheaters by focusing on three main aspects: analyzing the player’s point of view, statistically evaluating the player’s performance, and assessing the player’s gaming sense and performance consistency. Based on these aspects, we design structured and temporal features that accurately represent player behaviors. HAWK reproduces the human identification process using Long Short-Term Memory (LSTM) and attention mechanisms, ensemble learning, and deep learning networks, respectively.

We evaluate HAWK on a mainstream FPS game, CS:GO. To the best of our knowledge, this paper is the first server-side work using a substantial volume of real-world datasets with different cheat types and levels of sophistication, making HAWK and the datasets more convincing for industrial use. Specifically, our dataset includes 2,979 *aimbots* and 2,971 *wallhacks*, totaling 56,041 players. The scale of the dataset has increased by two orders of magnitude compared to the state-of-the-art work [9]. HAWK achieves a maximum of 84% recall and 80% accuracy in detecting both *aimbots* and *wallhacks*, outperforming the official in-use anti-cheat. It successfully identifies cheaters who had evaded previous detections and those never caught by the official systems. We created a demo website¹ to showcase some escapees’ illegal actions. HAWK validates its robustness against cheat evolution (introduced in Section 6.7) in real-world scenarios and showcases acceptable overheads. We particularly discuss HAWK’s generalizability in Section 7. The contributions of our work are as follows.

- Innovative anti-cheat observations and feature designs.
- Novel framework HAWK and a supporting workflow.
- Real-world evaluations with strong performance.
- Open-source HAWK and dataset² for future research.

2 Background

This section introduces anti-cheat and cheating techniques, replay systems, and replay files in modern FPS games.

¹Demo website. This is an anonymous website.

²Link. The repository and dataset will be released upon acceptance. Artifacts are uploaded for the reference. Ethics statement is shown in Section 10.

2.1 Server-side and Client-side Anti-Cheat

Client-side anti-cheats focus on data, process, and hardware protection [49, 58], or detection by either examining the existing cheats’ signatures [3, 22] or classifying through behavior [9]. However, attackers can bypass it with higher privileges, by sniffing the detection report through side-channel attack [23] and altering them in the transport layer, or by changing the program’s signature [35].

Server-side anti-cheats [2, 24, 39, 69, 70] emphasize data analysis and anomaly detection. Although the cheater’s inputs might be altered on the client, the cheaters must ensure their performance outperforms others to secure the win. Thus, it is easier to detect cheats on the server because it records all clients’ final-state actions that influence the gameplay. But the prior works have limitations mentioned in Section 1.

2.2 Cheat Types in FPS Games

Wallhack and aimbot are the two most prevalent types of cheats in FPS games [1]. Both types of cheats are mainly done by accessing the client’s memory data or image information. **Wallhack** enables players to visually penetrate obstructions like walls, which allows players to spot opponents across the map and effortlessly track their movements, providing a significant tactical advantage. **Aimbot** assists a player’s aims and shots so that the cheaters gain transcendent precision and reaction speed. *Aimbot*’s functionality can be customized according to player preference, allowing one to obtain different aiming performance, ranging from brutal-force aims to smooth aims like human [9]. *Aimbot* can be subdivided into *pure aimbot* (the primitive *aimbot*), *triggerbot* (auto-shoot only when the cross-hair is on the opponent), *micro-settings* (counteract recoil with Hotkeys), and *computer-vision-based aimbot* (aim with object detection models). In the following sections, *aimbot* refers to all aforementioned subcategories.

Notably, cheating provides different levels of sophistication [66]. The cheater might cheat cautiously, pretending to be a normal player, switching the cheat on and off, or cheating unabashedly with different configurations, various brands of cheating software, and categories. However, cheaters’ behaviors will always differ from the normal players [9]. Thus as long as cheaters want to gain unfair advantages, they must outperform the average. This is bound to create anomalies at the data level and therefore should be identifiable by models. Our evaluations in Section 6 include different levels of cheating sophistication by using large real-world datasets.

2.3 Replay System and Replay File

Replay system is a dynamic toolset for player interaction with recorded content post-game and has been extensively adopted in notable FPS games. Unlike video recordings, this system enables users to explore various perspectives, adjust

camera angles, and control playback speed for analysis by reconstructing the match with the *replay file*. **Replay file** refers to a comprehensive record of a match, encapsulated in a unique data format that can be interpreted by the *replay system*. **Demo** denotes the *replay file* in CS:GO. HAWK innovatively utilizes *demo* to extract data and avoid concurrent overheads on the server. We believe the *replay file* can be used as a novel data source for FPS server-side anti-cheat.

3 Overview

This section provides the key observations on the human experts' identification process and the workflow of HAWK.

3.1 Fact Observations

Although the anti-cheat tasks are still challenging for automation systems in not just the FPS field but almost any game genre, the illegal activities are identifiable for seasoned human players [11]. Therefore, by harnessing such inspiration, we discovered three observations that human experts always focus on to identify cheaters.

Observation 1 (OBS.1). Review a player's point-of-view (POV).

Akin to watching a player's game replay unfold over time, this review process involves analyzing various in-game behaviors, such as aim and shot, positioning and movement, and the in-game economy management and props utilization. These behaviors can provide temporal insights into whether the player is legitimately playing the game.

Observation 2 (OBS.2). Conduct an in-depth analysis of a player's statistical data.

Cheaters often exhibit statistical anomalies that set them apart from normal players. These anomalies include abnormally high accuracy and eliminations, a low death rate, and a high number of kills made through obstacles, etc. These statistical deviations serve as strong indicators of cheating.

Observation 3 (OBS.3). Examine the consistency between a player's game sense and combat performance.

A player requires substantial game experience to have better performances, which results in a positive correlation between a player's game sense and their performance. Thus, the inconsistency between the two aforementioned factors indicates potential cheating. For instance, if a player moves like a rookie but shoots and aims incredibly accurately, it is suspicious.

3.2 HAWK's Workflow

Figure 1 illustrates HAWK's workflow, comprising four inter-linked stages.

Stage One. Preprocessing. The *demo* is applied to parse in-game data from the banned databases. The multi-view features are then extracted from parsed data and then annotated for training. We discuss the feature constructions in Section 4.

Stage Two. HAWK deployment. HAWK utilizes the extracted features as inputs for its subsystems REVPOV (Section 5.1), REVSTATS (Section 5.2), and ExSPC (Section 5.3) to mimic human identification process, respectively. The outputs are incorporated into MVIN subsystem (Section 5.4) that presents a final cheating report.

Stage Three. Game Master (GM) team verification. Given the potential personal assets tied to a player's account, a ban should not be issued solely based on an algorithmic verdict. It is imperative to provide substantial evidence before initiating such an action. Hence, the final verdict requires GMs' verification to avoid false bans.

Stage Four. Data updates. Upon the affirmation of cheating, the relevant *replay files* are added to the banned databases. This act enriches and updates the reservoir of training samples which may contain novel patterns and behaviors. Thus, four stages constitute a cyclical workflow, with each stage contributing to the subsequent one.

This ongoing cyclical workflow enhances the system's robustness and provides a dynamic solution to multi-type cheat detection. We further discuss this in Section 6.7

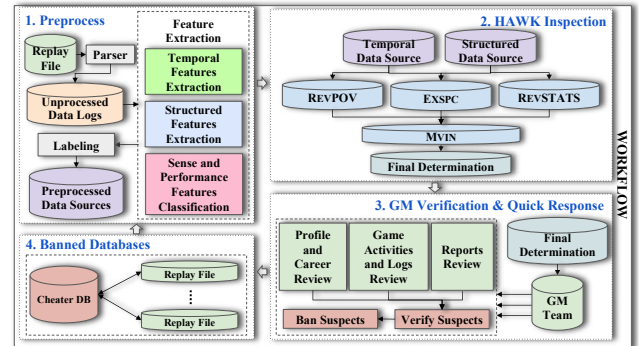


Figure 1: Cyclical workflow of HAWK.

4 Feature Constructions

The feature design is one of our contributions and key to the server-side anti-cheat. This section introduces the construction of temporal features, structured features, and the classification of sense and performance features. These features are intended to be a comprehensive representation of the three aspects of human identification of cheating in Section 3.1.

4.1 Temporal Features

Temporal features are information derived from the *demo* in the time domain. Each temporal data tuple represents the state information (e.g., coordinates, view directions, events, etc.) associated with the present *tick*. Where **tick** denotes the smallest unit of time in the game. This section describes temporal features' components and illustrates the distinctions in temporal features between normal players and cheaters.

4.1.1 Temporal Features Construction

According to different in-game behaviors, temporal features are segmented into three main categories and subdivided into seven specific types. This overview provides only categories and types due to the less-expressive nature of temporal features. [Appendix B](#) lists elaborate descriptions.

- **Engagement features** describes in-game engagement events, which are subcategorized into five types as follows.
 - **Damage features** indicate damage-inflicting events, including the occurring *tick*, the attacker's and victim's locations, view directions, weapons, damage value, etc.
 - **Auxiliary props features** related to auxiliary props utilization events (e.g., flashbang), including the deploy *tick*, victim's affected duration, etc.
 - **Offensive props features** related with events involving props that aid the attack (e.g., grenade, incendiary, etc.) including the deploy and destroy *ticks*, the props' type, the props' coordinates, etc.
 - **Elimination features** describes kill-related events, including the occurring *tick*, attacker's weapon and location, victim's location and view direction, etc.
 - **Weapon fire features** denotes firing-related occurrences, including the occurring *tick*, the weapon information, the shooter's location and view direction, etc.
- **Movement features** represents in-game positioning, mobility, and boolean flags per *tick*. For instance, coordinates, view directions, velocities in three dimensions, flags that indicate if the player is ducking, blinded, reloading, etc.
- **Economy features** reflects in-game financial aspects. For example, they include the equipment value and balance per *round* for each player.

4.1.2 Temporal Data Comparative Visualization

[Figure 2](#) comparatively analyzes the temporal features between cheaters and normal players across one *round*. Where **round** denotes the unit determining each win-loss outcome. One match has multiple rounds, and the players who win more rounds are the winners. In this example, there are four differences between cheaters and normal players. First, since the cheaters illegally acquire their opponents' position, the timing of cheaters' firing (pink) and engaging (red) highly overlap

(a). Second, normal players stay on guard (blue) irregularly to check for potential enemy locations, whereas cheaters are often on guard just before engagement (b). Third, normal players deploy props (orange) to gain a gunfighting or positional advantage, whereas cheaters rarely do so because they already have illegal advantages (c). Fourth, cheaters are rarely vulnerable (yellow) during the fire or engagement because they know the enemy's location and therefore can circumvent it in advance (d).

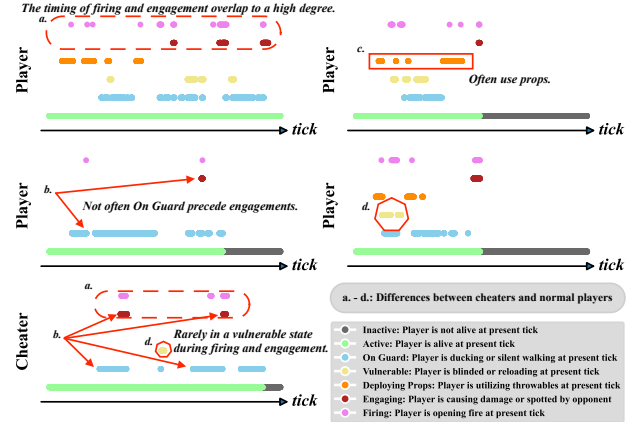


Figure 2: Comparative behavioral visualization between honest players and cheaters with respect to time scales.

4.2 Structured Features

Structured features are single-value data calculated with well-designed algorithms to represent integrated in-game behavioral information per match. This section describes the components of structured features and visualizes the structured feature differences between normal players and cheaters.

4.2.1 Structured Features Construction

The structured features for HAWK are categorized into four main categories that comprise 28 strong-expressiveness features. For the sake of brevity and coherence, only the introduction of categories is outlined below. A meticulous breakdown can be referred to in [Appendix C](#).

- **Aiming features** represents the efficiency and efficacy of aims. We break down the aiming process into three moments (initial spot, first-time fire, and first-time hit) and two stages (reaction and adjustment). We extract different elapsed durations and angle variations with statistical representations (e.g., average or variance) to indicate the player's different performances within a match. For example, the average of *reaction duration* reflects a player's level of reaction speed, and the variance of that denotes the distribution of the reaction duration. Typically, in terms of

the reaction stage, normal players obtain a higher mean value and more diverse variance compared with cheaters.

- **Firing features** reflects shot proficiency. For example, the *hit group distribution variance* describes the dispersion of body part that suffers damage for the current player in a match. Most cheaters with *aimbot* prefer to lock on specific *hit group* (i.e., *head*) to achieve faster elimination.
- **Elimination features** emphasizes metrics related to in-game eliminations or kill-focused activities. For example, the *occluder-penetration index* is a weighted index that reflects the extent of the average occluder-penetration eliminations (e.g., eliminate the opponent behind walls or smoke) conducted by the player. In terms of the cheaters exploiting *wallhacks*, this index is more significant than the normal players’.
- **Props utilization features** captures a player’s adeptness at using in-game auxiliary and offensive props like flashbang, grenades, etc. For instance, the *props utilization index* denotes how frequently a player utilizes auxiliary and offensive props such as incendiaries and smoke grenades. This can help distinguish a player’s familiarity with the game and their skillfulness.

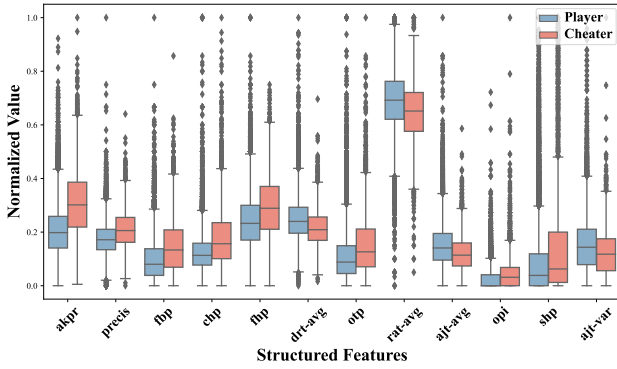


Figure 3: Box plots of comparative visualization between honest players and cheaters on top-12 structured features under Mann-Whitney U (Wilcoxon Rank-Sum) test with P-Value ascending (distinction descending) order.

4.2.2 Structured Data Comparative Visualization

Figure 3 offers a box-plot on structured features to analyze between honest players and cheaters comparatively. Each feature on the x-axis (we select top-12 features for illustration purposes) is ordered based on the outcomes of the Mann-Whitney U test, with the leftmost features, such as *akpr* (introduced in Appendix C), marking pronounced disparities between the two groups. This implies that features towards the left end, showcased by their lower p-values, are more distinguishable, whereas those on the right are less so. The y-axis

is normalized values between 0 and 1. The box plots, differentiated by blue for honest players and orange for cheaters, provide insights into the median, interquartile range, and outlier distributions. In which, diamond shapes represent outliers, emphasizing the spread and distribution of data across the features. Despite considering dimensionality reduction techniques, such as PCA (Figure 13), empirical tests show an optimal performance when all 28 features were employed.

4.3 Sense and Performance Features

Sense and performance features are derived from the two subsections above. Appendix D includes detailed classification.

- **Sense features** denote a player’s in-game cognition, reflecting strategic understanding, and tactical anticipation.
 - **Temporal sense features** include temporal features that reflect a player’s gaming sense such as economic considerations, movement dynamics, grenade usage, etc.
 - **Structured sense features** contain structured features that describe in-game understanding, e.g., flash efficiency, prop utilization, etc.
- **Performance features** demonstrate in-game efficacy, indicating engagement capabilities, precision in aiming, and mastery over game mechanisms.
 - **Temporal performance features** include temporal features that indicate continuous in-game performances, e.g., eliminations, damage, weapon proficiency, etc.
 - **Structured performance features** contain the remaining structured features that statistically describe the player’s in-game performances, such as time to kill, elimination-related features, etc.

5 HAWK

To mimic human experts’ identification process, we propose HAWK which consists of four subsystems: Review Point-of-View (REVPOV) subsystem, Review Statistics (REVSTATS) subsystem, Examine Sense-Performance Consistency (EXSPC) subsystem, and Multi-View Integration (MVIN) subsystem. The first three subsystems’ designs are associated with the three observations we discovered regarding the inherent nature of the cheat identification process as elaborated in Section 3.1. The fourth subsystem integrates the results derived from the first three subsystems.

5.1 REVPOV

Aligned with **OBS.1**, REVPOV thoroughly examines a player’s time-series operations within a match.

Multi-LSTM Attention Encoders: In Figure 4 (a), we feed the seven sets of temporal features (Section 4.1.1) as input to

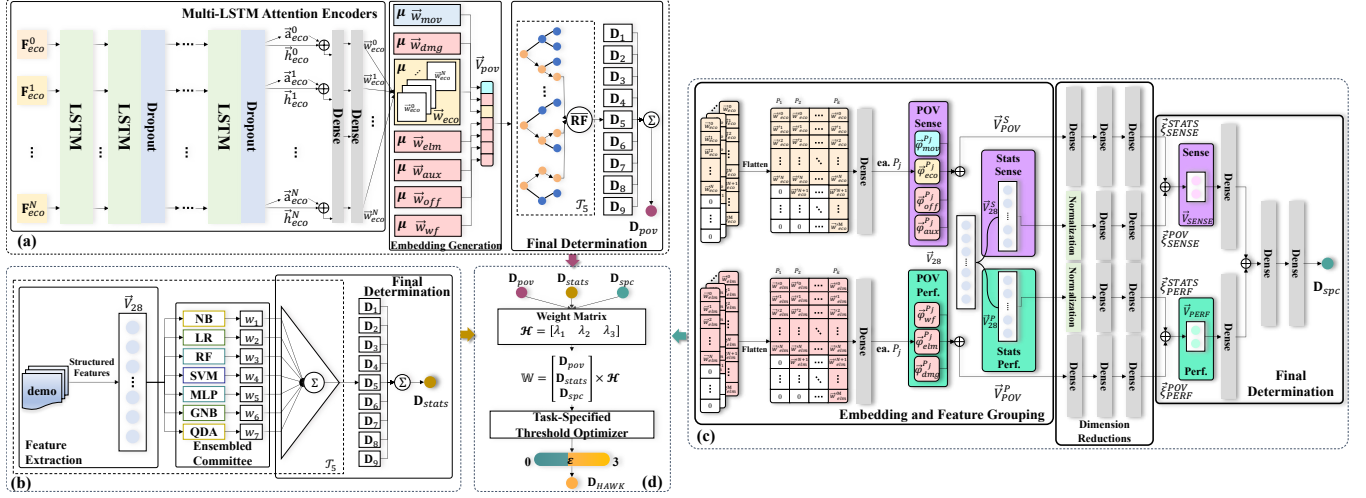


Figure 4: HAWK framework illustration. (a)-REVPOV, (b)-REVSTATS, (c)-ExSPC are corresponding to three observations in Section 3.1, (d)-MVIN is an integration network for combining the determinations from the aforementioned three subsystems.

seven independent Long Short-Term Memory (LSTM) [29] networks to acquire the embeddings. For explanatory purposes, we illustrate the process using the example of the *Economy* features. $\mathbf{F}_{\text{eco}}^n$ denotes the input feature vector. A dropout layer [54] is employed from the second to last LSTM layers respectively to mitigate the risk of overfitting. \vec{h}_G^n denotes the output of the encoder, consists of one set of the seven temporal features mentioned in Section 4.1.1, where G represents the set and n indicates the sequence number among all outputs. For each time step, we introduce the Luong-style attention [41] afterward to help the model better understand the importance of different positions in the input sequence and aggregate different parts of the input weights. In Equation 1, a_G^i represents the attention weight for the time step i . \mathbf{W}_q and \mathbf{W}_k denotes the learned weight matrices of *query* and *key* in attention mechanism. i, j and k indicate different time steps. Concatenation operation is executed afterward, yielding $[\vec{d}_G^n || \vec{h}_G^n]$, where $||$ denotes concatenation. After two dense layers, \vec{w}_G^n represents the final tensor for binary classification.

$$\vec{a}_G^i = \sum_{j=0}^N \frac{\exp(\mathbf{W}_q \cdot \vec{h}_G^i) \cdot (\mathbf{W}_k \cdot \vec{h}_G^j)}{\sum_{k=0}^N \exp(\mathbf{W}_q \cdot \vec{h}_G^i) \cdot (\mathbf{W}_k \cdot \vec{h}_G^k)} \cdot \vec{h}_G^j \quad (1)$$

Embedding Generation: An average pooling is conducted to flatten the output sequence. Equation 2 indicates the average operation, where N denotes the number of output sequences. \vec{v}_{pov} is used as embedding for the final determination.

$$\vec{w}_G = \frac{\sum_{n=0}^N \vec{w}_G^n}{N+1} \quad (2)$$

$$\vec{v}_{pov} = [\vec{w}_{\text{eco}} || \vec{w}_{\text{mov}} || \vec{w}_{\text{dmg}} || \vec{w}_{\text{elm}} || \vec{w}_{\text{aux}} || \vec{w}_{\text{off}} || \vec{w}_{\text{wf}}] \quad (3)$$

Final Determination: In the context of cheat detection, the dataset often exhibits a class imbalance, where the majority

of players are honest, inadvertently leading to biased learning towards the dominant class. Therefore, we adopt a *multi-subsampling* strategy to level the playing field for the minority class, creating balanced representations of both cheating and honest behaviors. Suppose \mathcal{T} is the initial training set. To establish a balanced class distribution, we perform a selective sampling on \mathcal{T} , specifically targeting the honest player samples. We perform this operation nine times in accordance with the ratio of honest to dishonest players, generating nine distinct training sets, each denoted as \mathcal{T}_k , where k indicates the iteration count. Conduct each iteration of the sampling process to select unique honest player samples, thereby adding varied examples to the learning process. Subsequently, we obtain nine separately trained Random Forest models, each corresponding to one of the diversified and balanced training sets \mathcal{T}_k , we named this strategy as *multi-forest*. The averaging method in Equation 4 is selected for REVPOV final class prediction. Consider a random forest consisting of N decision trees, each producing a prediction denoted as $h_i(\vec{V}_{pov}^k)$, where i indicates the i -th tree, k denotes the k -th sampled set, and \vec{V}_{lstm} represents the input feature vector. The prediction of each tree is a probability distribution, indicating the likelihood of the sample \vec{V}_{pov}^k belonging to each class. p_i represents the probability that the i -th tree predicts sample \vec{V}_{pov}^k to be in class j . In Equation 4, $\overline{\text{RF}}(\vec{V}_{pov}^k)$ denotes the average prediction output of the random forest, which is the average of the prediction probability vectors of all decision trees. The prediction for each \vec{D}_k can be obtained by selecting the class with the highest predicted probability shown in Equation 5, where $(\overline{\text{RF}}(\vec{V}_{pov}^k))_j$ represents the probability of class j in $\overline{\text{RF}}(\vec{V}_{pov}^k)$. After the *multi-forest*, we acquire the corresponding determination \mathbf{D}_k . Lastly, as in Equation 6, we obtain the final classification determination \mathbf{D}_{pov} for REVPOV.

$$\overline{\mathbf{RF}}(\vec{V}_{pov}^k) = \frac{1}{N} \sum_{i=1}^N h_i(\vec{V}_{pov}^k) = \frac{1}{N} \sum_{i=1}^N \mathbf{p}_i \quad (4)$$

$$\mathbf{D}_k = \arg \max_j \left(\overline{\mathbf{RF}}(\vec{V}_{pov}^k) \right)_j \quad (5)$$

$$\mathbf{D}_{pov} = \arg \max_j \sum_{k=1}^9 \mathbf{D}_k^{(j)} \quad (6)$$

5.2 REVSTATS

Aligned with **OBS.2**, REVSTATS subsystem is designed to perform an in-depth analysis of structured features to capture the cheaters. Cheaters often exhibit deviations in their static data compared to normal players. Even when cheaters deliberately attempt to conceal their behavior, the subtle differences tend to accumulate over time and reveal disparities in the statistical data post-game.

Feature Extraction: In Figure 4 (b), \vec{V}_{28} denotes the vector representation of the structured features (Section 4.2.1).

Ensembled Committee: We empirically use seven classifiers [7, 13, 14, 28, 34, 46, 55] in an ensembled way. Each model is independently trained. Upon completion, each model independently adjudicates each test sample. The outputs are binary signifying the presence or absence of cheating.

Final Determination: Due to imbalanced dataset, a similar *multi-subsampling* strategy as employed in the REVPOV subsystem is adopted for the REVSTATS subsystem to fully leverage the available data without losing valuable information. For each classification model, we generate a distinct model for each subsampled set. Each model provides an individual prediction. A majority voting scheme is utilized within each classification algorithm to aggregate the results of the nine models. The final determination is also achieved through the majority voting mechanism, which collates the determinations from all seven classification algorithms. In Equation 7, where \mathbf{D}_{stats} signifies the binary final determination. Where w_j denotes the decision from the j th classification algorithm, and $I(\cdot)$ is the indicator function, returning 1 if the condition within the brackets is true, and 0 otherwise. The decision, i , which receives the majority of votes from all seven classification algorithms, is accepted as the final determination.

$$\mathbf{D}_{stats} = \arg \max_{i \in \{0,1\}} \sum_{j=1}^7 I(w_j = i) \quad (7)$$

5.3 ExSPC

Aligned with **OBS.3**, ExSPC subsystem is designed to inspect a comprehensive investigation of the consistency of a player's in-game senses and overall performances.

Embedding and Feature Grouping: There are seven embeddings and two groups of vectors as input (Section 4.3) in ExSPC, in which seven embeddings are generated by using the trained models in REVPOV and two vectors are the subsets

of \vec{V}_{28} in REVSTATS. Each embedding is padded to the maximum length of that in the whole dataset. \vec{w}_G^k is the intermediary result from REVPOV, where k represents the numbering in the sequence, G denotes the type of the temporal features. Each embeddings are represented in two-dimensional arrays. In Figure 4 (c), P_1 to P_k indicates different players, we exemplify with one player P_j . Therefore, we flatten the embeddings into one-dimensional arrays and use a dense layer with an *ELU* activation function to shrink the dimensions. After the seven different similar groups of layers, we obtain φ_G^j . Subsequently, we divide seven different types of tensors as shown in Appendix D, and concatenate each group of tensors for each player. In which, sense vector of the temporal features is $\vec{V}_{POV}^S = [\varphi_{mov}^{P_j} || \varphi_{eco}^{P_j} || \varphi_{off}^{P_j} || \varphi_{aux}^{P_j}]$ and performance vector of the temporal features is $\vec{V}_{POV}^P = [\varphi_{wf}^{P_j} || \varphi_{elm}^{P_j} || \varphi_{dmg}^{P_j}]$. In terms of two vectors, we also divided \vec{V}_{28} into two groups according to Appendix D, namely the sense vector of structured features \vec{V}_{28}^S and the performance vector of structured features \vec{V}_{28}^P .

Dimension Reduction: \vec{V}_{28}^S and \vec{V}_{28}^P are normalized at first. Afterward, each group of the four vectors goes through different groups of dense layers to reduce the dimensions. Next, we concatenate four vectors and yield two vectors eventually representing sense $\vec{V}_{SENSE} = [\vec{\zeta}_{SENSE}^S || \vec{\zeta}_{SENSE}^P]$ and performance $\vec{V}_{PREF} = [\vec{\zeta}_{PREF}^S || \vec{\zeta}_{PREF}^P]$ respectively.

Final Determination: When acquiring \vec{V}_{SENSE} and \vec{V}_{PREF} , we further reduce its dimension and deepen the network for better learning performances. Then, we concatenate two vectors and go through one final dense layer for reducing the dimension and another dense layer with sigmoid activation function for binary classification. Eventually, the final classification determination \mathbf{D}_{spc} for ExSPC subsystem is obtained. The class weight is set as one to nine like previous subsystems. Both REVPOV and ExSPC use *Binary Cross-Entropy* as loss function shown in Equation 8, where N represents the number of samples, y_i is the true label of the i -th sample, \hat{y}_i is the predicted value for the i -th sample.

$$\text{Loss} = -\frac{1}{N} \sum_{i=1}^N [y_i \log(\hat{y}_i) + (1 - y_i) \log(1 - \hat{y}_i)] \quad (8)$$

5.4 MVIN

In Figure 4 (d), MVIN is to harness the collective determinations from REVPOV, REVSTATS, and ExSPC. By integrating the predictions from these subsystems, MVIN aims to deliver a final verdict regarding a player's cheating disposition.

Data Integration: The subsystem integrates the outcomes from REVPOV, REVSTATS, and ExSPC, symbolized as \mathbf{D}_{pov} , \mathbf{D}_{stats} , and \mathbf{D}_{spc} . Given the diverse nature of these outputs, a structured preprocessing phase becomes indispensable. This step is designed to merge the individual outputs and synchronize them for the succeeding integration process.

Model Optimization: MVIN adopts a weight matrix for each subsystem’s determination, where weights are assigned based on the subsystem’s importance and reliability. The weighted output, \mathbb{W} , is calculated as [Equation 9](#). Where λ_1 , λ_2 , and λ_3 represent the weights associated with the outputs of the subsystems REVPOV, REVSTATS, and ExSPC, respectively.

$$\mathbb{W} = \lambda_1 \cdot \mathbf{D}_{pov} + \lambda_2 \cdot \mathbf{D}_{stats} + \lambda_3 \cdot \mathbf{D}_{spc} \quad (9)$$

Final Determination: Once \mathbb{W} is calculated, it then undergoes thresholding via the *Task-Specified Threshold Optimizer*. This optimizer is to provide a binary determination based on a specified threshold ϵ . The exact nature of this threshold optimizer, whether it leans towards recall, accuracy, or other metrics can be set based on user or system requirements. For instance, in a recall-focused setting, the optimizer would aim to identify every potential cheater, accepting the risk of higher false positives. Conversely, in an accuracy-driven mode, the optimizer would aim to reduce false positives, even if it means potentially missing some cheaters. This threshold ϵ therefore acts as a decision boundary, converting the continuous weighted value \mathbb{W} into a discrete binary outcome \mathbf{D}_{HAWK} . By harnessing the strengths of each subsystem and compensating for their inherent limitations, MVIN is crucial to integrate determinations from different subsystems. *Task-Specified Threshold Optimizer* offers Game Masters (GM) a degree of selectivity, enabling them to fine-tune the system based on the desired anti-cheat needs.

6 Experiments

We conduct experiments to answer six research questions (**RQ.1–RQ.6**):

- **RQ.1:** What are the performances of HAWK and each subsystem? ([Section 6.4](#))
- **RQ.2:** Compared to the current official inspection, to what extent HAWK has improved in terms of effectiveness and efficiency? ([Section 6.5](#))
- **RQ.3:** What are the performances of HAWK under different settings of the *Task-Specified Threshold Optimizer*? ([Section 6.6](#))
- **RQ.4:** What is the robustness of HAWK and its subsystems against cheat evolution? ([Section 6.7](#))
- **RQ.5:** Is there any suspicious activity that still exists but has never been detected by officials? ([Section 6.8](#))
- **RQ.6:** What are the overheads of HAWK’s subsystems? ([Section 6.9](#))

6.1 Incomparability to Prior Works

First, most prior works [2, 24, 39, 69–71] are not open-sourced. Second, data collection method is distinct and incompatible. HAWK utilizes the *replay file* post-game, which differs fundamentally from prior studies that modified the game engine

or applied mods during gameplay. Third, the installation on commercial clients or servers is infeasible. If the installation of the prior works is implemented before the commencement of data collection, the data can then be gathered and evaluated. However, the *demos* we collected come directly from the game platform, which prohibits the installation of any unverified programs on clients or servers due to legal constraints. In addition to the aforementioned reasons with commonality, we also further state below the specific reasons for the detailed incomparability between HAWK and the SOTA designs. There are three aspects of incomparability with BotScreen [9]. First, CS:GO has gone through several major patch updates after BotScreen was released. The authors of BotScreen confirmed through email that BotScreen, as well as Osiris [37] (the identical cheat used in BotScreen for feature extraction and evaluation), does not apply to the in-use version of games. Second, the deprecation of Intel SGX [5, 31] prevents us from conducting comparative experiments. Third, it can only detect *pure aimbot*, making the comparison less significant. Black-Mirror [49] and Invisibility Cloak [58] are prevention designs only for counteracting *wallhacks* and *computer-vision-based aimbots* respectively. Both studies are only functional before the cheats happen. Whereas HAWK and other prior works are detection systems that functional post-cheating.

Table 1: Dataset separation and description.

CT ¹	Train				Validation				Test			
	#M ²	#P ³	#N ⁴	#C ⁵	#M ²	#P ³	#N ⁴	#C ⁵	#M ²	#P ³	#N ⁴	#C ⁵
Aimbot	1,009	10,127	9,150	977	975	8,561	7,697	864	995	9,047	8,163	884
Wallhack	833	8,320	7,500	820	1,037	9,712	8,745	967	1,101	10,274	9,249	1,025

¹CT: Cheat type; ²#M: Number of matches; ³#P: Number of players in total; ⁴#N: Number of normal (honest) players; ⁵#C: Number of cheaters.

6.2 Experimental Settings and Ground Truth

The *demos* are open-sourced and acquired from a well-known and recognized CS:GO platform³. The initial data extraction utilizes an open-source library *awpy* [67] to parse the raw data in *demos* into JSON files, which contain comprehensive information for the following feature constructions.

[Table 1](#) is the dataset description. [Figure 5](#) illustrates the experiments’ process. We evaluate HAWK with two of the most prevalent cheat types, *aimbot* and *wallhack*. For *aimbot*, we set one collection window (16 days in total). For *wallhack*, we set two collection windows (27 days in total, we explain the reason for window inconsistency in [Section 6.7](#)). All *demos* are real-world ranking matches within the collection windows. Therefore, the cheats used by the player are black-boxes for anti-cheating. Both datasets contain different levels of cheating sophistication.

The dates of cheaters’ label acquisition both end on the last day of data collection in each set (i.e., *first labeling*),

³Link. We anonymize the platform’s URL and name

Table 2: Ablation study results on each of the subsystems.

CT ¹	System	Validation										Test									
		TP	TN	FP	FN	Accuracy	Recall	NPV	AUC-ROC	OEI ²	TP	TN	FP	FN	Accuracy	Recall	NPV	AUC-ROC	OEI ²		
Aimbot	REVPOV	458	4,796	2,901	406	0.614	0.530	0.922	0.577	1.246	481	5,088	3,075	403	0.616	0.544	0.927	0.584	1.283		
	REVSTATS	453	7,290	407	411	0.904	0.524	0.947	0.736	4.941	566	6,797	1,366	318	0.814	0.640	0.955	0.736	2.864		
	ExSPC	553	6,187	1,510	311	0.787	0.640	0.952	0.779	2.529	558	6,616	1,547	326	0.793	0.631	0.953	0.786	2.586		
	HAWK	614	5,803	1,894	250	0.750	0.711	0.959	0.732	2.326	642	5,837	2,326	242	0.716	0.726	0.960	0.721	2.126		
Wallhack	REVPOV	573	6,081	2,664	394	0.685	0.593	0.939	0.644	1.670	627	6,364	2,885	398	0.680	0.612	0.941	0.650	1.684		
	REVSTATS	604	8,241	504	363	0.911	0.625	0.958	0.783	4.143	855	6,988	2,261	170	0.763	0.834	0.976	0.795	1.946		
	ExSPC	760	7,258	1,487	207	0.826	0.786	0.972	0.885	3.303	501	8,484	765	524	0.875	0.489	0.942	0.840	3.736		
	HAWK	798	7,033	1,712	169	0.806	0.825	0.977	0.815	3.118	869	6,902	2,347	156	0.756	0.848	0.978	0.797	2.649		

¹CT: Cheat type; ²OEI: Operational Efficiency Index.

Table 3: Comparison result on the different model selection of REVSTATS.

CT ¹	Model	Validation										Test									
		TP	TN	FP	FN	Accuracy	Recall	NPV	AUC-ROC	OEI ²	TP	TN	FP	FN	Accuracy	Recall	NPV	AUC-ROC	OEI ²		
Aimbot	LogisticRegression	570	6,204	1,493	294	0.791	0.660	0.955	0.733	2.614	713	4,897	3,266	171	0.620	0.807	0.966	0.703	1.772		
	Naive Bayes	467	6,740	957	397	0.842	0.874	0.944	0.708	3.069	625	5,928	2,235	259	0.724	0.707	0.958	0.717	2.143		
	RandomForest	415	7,694	3	449	0.947	0.480	0.945	0.740	4.313	427	7,634	529	457	0.891	0.483	0.944	0.709	4.313		
	SVM	309	7,615	82	555	0.926	0.358	0.932	0.673	7.299	405	7,665	498	479	0.892	0.458	0.941	0.699	4.320		
	MLP	858	7,697	0	6	0.999	0.993	0.999	0.997	9.901	508	7,325	838	376	0.866	0.575	0.951	0.736	3.674		
	GaussianNB	467	6,740	957	397	0.842	0.541	0.944	0.708	3.069	625	5,928	2,235	259	0.724	0.707	0.958	0.717	2.143		
	QDA	350	7,181	516	514	0.880	0.405	0.933	0.669	3.737	534	6,770	1,393	350	0.807	0.604	0.951	0.717	2.697		
	REVSTATS	453	7,290	407	411	0.904	0.524	0.947	0.736	4.941	566	6,797	1,366	318	0.814	0.640	0.955	0.736	2.864		
Wallhack	LogisticRegression	714	7,629	1,116	253	0.859	0.738	0.968	0.805	2.861	943	5,622	3,627	82	0.639	0.920	0.986	0.764	1.420		
	Naive Bayes	604	7,677	1,068	363	0.853	0.625	0.955	0.751	2.741	891	6,103	3,146	134	0.681	0.869	0.979	0.765	1.545		
	RandomForest	967	8,745	0	1	1.000	1.000	1.000	1.000	6.713	751	8,083	1,166	274	0.860	0.733	0.967	0.803	2.872		
	SVM	548	8,323	422	419	0.913	0.567	0.952	0.759	4.378	817	7,227	2,022	208	0.783	0.797	0.972	0.789	2.065		
	MLP	472	8,489	256	495	0.923	0.488	0.945	0.729	5.186	788	7,726	1,523	237	0.829	0.769	0.970	0.802	2.471		
	GaussianNB	604	7,677	1,068	363	0.853	0.625	0.955	0.751	2.741	891	6,103	3,146	134	0.681	0.869	0.979	0.765	1.545		
	QDA	493	8,276	469	474	0.903	0.510	0.946	0.728	4.057	815	7,270	1,979	210	0.787	0.795	0.972	0.791	2.095		
	REVSTATS	604	8,241	504	363	0.911	0.625	0.958	0.783	4.143	855	6,988	2,261	170	0.763	0.834	0.976	0.795	1.946		

¹CT: Cheat type; ²OEI: Operational Efficiency Index.

this label is used for training and most of the evaluations in Figure 5. The official inspections are continuous, including multiple industry-in-use proprietary closed-source anti-cheats and manual checks. The officials update the ban list daily. However, due to the long ban cycle of the official inspections, most cheaters will not get banned on the day they cheat. Therefore, after 65 days of the *first labeling*, we once again acquired the labels (i.e., *second labeling*) of the whole datasets to screen out cheaters who had not been labeled correctly in the *first labeling* for further analysis on the false positives (the increased cheater numbers are shown in Table 4).

Although the two datasets contain different types of cheat, the official in-use anti-cheats can not label the specific subcategories, but can only annotate the broad categories of cheats. Cheating sophistication is subjective and difficult to quantify. Hence, even though we want to provide further information, it is infeasible to provide a more detailed breakdown of the datasets. Besides, due to the low recall and accuracy of the current in-use anti-cheats, there will be inevitable noise (cheaters who have evaded the official anti-cheats) in the negative labels within the ground truth.

6.3 Evaluation Metrics

Our chosen evaluation metrics are more skewed towards reflecting how well the cheaters can be identified. We use the following metrics in Appendix F and *Operational Efficiency*

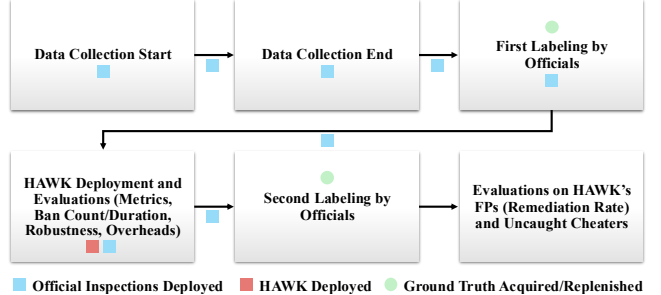


Figure 5: Experiments' process and labeling details.

Index (OEI) to distinguish between cheating and normal behaviors. *OEI* is a new metric for evaluating the efficiency of industrial operations. **Operational Efficiency Index (OEI)**, represented in Equation 10, where N represents the total number of players. It reflects the operational efficiency gains in manual review processes. A higher *OEI* indicates a greater reduction in manual verification and a more effective system.

$$OEI = \left(\frac{N}{TP + FP} \right) \cdot (Recall \cdot NPV) \quad (10)$$

6.4 Ablation Study Results

To answer **RQ.1**, we conduct an ablation study on HAWK shown in Table 2. We set the *Task-Specified Threshold Op-*

timizer to achieve the highest *accuracy* with at least 70% *recall* for detecting *aimbot*, and the highest *AUC-ROC* for detecting *wallhack*, illustrating different anti-cheat scenarios. Overall, HAWK excels in identifying authentic cheaters, evidenced by the highest *recall* and *NPV* across all evaluations. For *aimbot* detection, REVSTATS enhances *accuracy* by effectively filtering normal players in both validation and test sets. In *wallhack* detection, REVSTATS excels in the validation set, while ExSPC leads in the test set. Although some components like REVSTATS and ExSPC outperform HAWK in *accuracy*, their lower *recall* (up to 64%) limits their effectiveness, affirming HAWK as the optimal choice. Notably, the *Wallhack* dataset yields better overall performance than the *Aimbot* dataset. We believe this is due to the latter’s diverse subcategories of *aimbots*. In Table 5 and Table 3, we present REVPOV’s and REVSTATS’s model selection results among hundreds of tested models, and promising models are demonstrated. REVPOV outperforms other models with balanced, consistent accuracy and recall. Random Forest outperformed other models under the sampled data in REVPOV. Thus, we adopt *multi-forest* and *multi-subsampling* with Random Forest. REVSTATS outperforms individual classifiers in balancing recall and accuracy by capitalizing on the strengths of each classifier while mitigating their weaknesses. The training and validation loss for ExSPC in Figure 9 and Figure 10 (further discussed in Appendix A).

Table 4: The manual average ban duration comparison and the remediation rate among HAWK’s false positives after the first labeling.

CT ¹	HAWK ²	Off. ³	Validation			Test		
			#MTPs ⁴	Rmd% ⁵	#IncrPs ⁶	#MTPs ⁴	Rmd% ⁵	#IncrPs ⁶
Aimbot	~4 min	5.88 days	93	4.91%	237	97	4.17%	233
Wallhack	~4 min	4.47 days	93	5.43%	226	153	6.52%	303

¹CT: Cheat type;

²HAWK: The process time of HAWK varies with match length, HAWK’s detailed overheads are evaluated in Section 6.9;

³Off.: The average ban duration of official manual inspections per match;

⁴#MTPs: The number of missed true positives among the false positives;

⁵Rmd%: The percentage of #MTPs in the number of false positives;

⁶#IncrPs: The number of increased positives (cheaters) labeled by the officials after the second labeling.

6.5 HAWK and Official Inspection Comparison

To answer **RQ.2**, we calculate the daily number of bans for the day and cumulative ban-sums by HAWK and the official inspections illustrated in Figure 6. The figure indicates that HAWK’s identification effectiveness (daily count in red bars) and efficiency (cumulative count in red lines) outrank those of the official manual inspections (blue bars and lines) on both cheat types. Additionally, Table 4 compares the average ban duration per match, revealing that HAWK’s seconds-scale processing time is exponentially more efficient than official inspections. The remediation rate indicates the percentage

of cheaters not banned in the first labeling but caught in the second labeling. In Table 4, we list the remediation rate after the second labeling among HAWK’s false positives (which are obtained after the first labeling). It demonstrates that HAWK can capture the authentic cheaters among the *normal players* initially labeled by the official anti-cheats. This also suggests that while HAWK is robust to mislabeled data, using a purer dataset would further improve results.

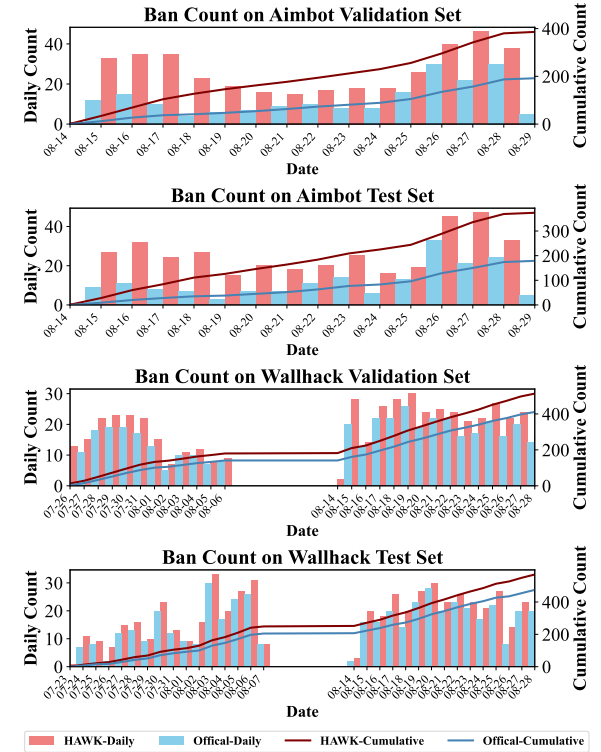


Figure 6: Daily number of bans for the day and cumulative ban-sums by HAWK versus the official manual inspections.

6.6 Analysis on Different MVIN Settings

To address **RQ.3**, we conduct a comparative analysis of HAWK under different MVIN settings, as shown in Table 6. The *Optimizer* column indicates the priority choices of the *Task-Specified Threshold Optimizer*, such as *F1-Score* for highest *F1-Score* and $Acc_{rc} > 0.75$ for highest *accuracy* with *recall* above 75%. An inevitable trade-off exists between capturing more cheaters and minimizing false positives due to cheating sophistication and dataset noise (Section 6.2). As discussed in Section 5.4, GMs can dynamically adjust optimizers, allowing for quick retraining of MVIN, with new weight matrices and thresholds generated in about one minute. This adaptability aligns with the varying intensity of required anti-cheat measures, offering flexibility in balancing performance and efficiency. GMs can use different optimizers to meet specific anti-cheat needs. Interestingly, GMs do not always aim to

Table 5: Comparison result on the different model selection of REVPOV. N/A in OEI indicates the denominator is 0.

CT ¹	Model	Validation										Test									
		TP	TN	FP	FN	Accuracy	Recall	NPV	AUC-ROC	OEI ²	TP	TN	FP	FN	Accuracy	Recall	NPV	AUC-ROC	OEI ²		
Aimbot	REPTree [21]	19	7,660	37	845	0.897	0.022	0.901	0.509	3.028	33	8,118	45	851	0.901	0.037	0.905	0.516	3.919		
	RandomTree	123	6,914	783	741	0.822	0.142	0.903	0.520	1.215	125	7,399	764	759	0.832	0.141	0.907	0.524	1.305		
	RseslibKNN [26]	40	7,460	237	824	0.876	0.046	0.901	0.508	1.289	33	7,868	295	851	0.873	0.037	0.902	0.501	0.929		
	SPAARC [68]	0	7,697	0	864	0.899	0.000	0.899	0.500	N/A	0	8,163	0	884	0.902	0.000	0.902	0.500	N/A		
	RandomForest	16	7,665	32	848	0.897	0.019	0.900	0.507	2.974	33	8,128	35	851	0.902	0.037	0.905	0.517	4.496		
	Bagging [6]	18	7,666	31	846	0.898	0.021	0.901	0.508	3.278	30	8,129	34	854	0.902	0.034	0.905	0.515	4.341		
	VFI [20]	822	445	7,252	42	0.148	0.951	0.914	0.505	0.922	848	472	7,691	36	0.146	0.959	0.929	0.509	0.944		
	JRip [10]	21	7,663	34	843	0.898	0.024	0.901	0.510	3.408	42	8,116	47	842	0.902	0.048	0.906	0.521	4.376		
	MODLEM [57]	19	7,588	109	845	0.889	0.022	0.900	0.504	1.323	34	8,029	134	850	0.891	0.038	0.904	0.511	1.873		
	CHIRP [65]	0	7,697	0	864	0.899	0.000	0.899	0.500	N/A	0	8,163	0	884	0.902	0.000	0.902	0.500	N/A		
Wallhack	CSForest [52]	50	7,292	405	814	0.858	0.058	0.900	0.503	0.980	58	7,755	408	826	0.864	0.066	0.904	0.508	1.151		
	REVPOV	458	4,796	2,901	406	0.614	0.530	0.922	0.577	1.246	481	5,088	3,075	403	0.616	0.544	0.927	0.584	1.283		
	REPTree	47	8,641	104	920	0.895	0.049	0.904	0.518	2.825	66	9,140	109	959	0.896	0.064	0.905	0.526	3.421		
	RandomTree	178	8,006	738	789	0.843	0.184	0.910	0.550	1.776	198	8,433	816	827	0.840	0.193	0.911	0.552	1.782		
	RseslibKNN	89	8,515	230	878	0.886	0.092	0.907	0.533	2.540	120	8,939	310	905	0.882	0.117	0.908	0.542	2.540		
	SPAARC	69	8,679	66	898	0.901	0.071	0.906	0.532	4.652	87	9,164	85	938	0.900	0.085	0.907	0.538	4.599		
	RandomForest	27	8,713	32	940	0.900	0.028	0.903	0.512	4.149	35	9,212	37	990	0.900	0.034	0.903	0.515	4.400		
	Bagging	26	8,705	40	941	0.899	0.027	0.902	0.511	3.571	37	9,201	48	988	0.899	0.036	0.903	0.515	3.940		
	VFI	950	563	8,182	17	0.156	0.982	0.971	0.523	1.014	1,008	689	8,560	17	0.166	0.983	0.976	0.529	1.031		
	JRip	36	8,670	75	931	0.896	0.037	0.903	0.514	2.941	71	9,179	70	954	0.900	0.069	0.906	0.531	4.572		
	MODLEM	35	8,687	58	932	0.898	0.036	0.903	0.515	3.414	56	9,171	78	969	0.898	0.055	0.904	0.523	3.789		
	CHIRP	6	8,738	7	961	0.900	0.006	0.901	0.503	4.176	8	9,242	7	1,017	0.900	0.008	0.901	0.504	4.816		
	CSForest	0	8,745	0	967	0.900	0.000	0.900	0.500	N/A	0	9,249	0	1,025	0.900	0.000	0.900	0.500	N/A		
	REVPOV	573	6,081	2,664	394	0.685	0.593	0.939	0.644	1.670	627	6,364	2,885	398	0.680	0.612	0.941	0.650	1.684		

¹CT: Cheat type; ²OEI: Operational Efficiency Index.

Table 6: HAWK detection result with different Task-Specified Threshold Optimizer settings.

CT ¹	Optimizer ²	Validation										Test									
		TP	TN	FP	FN	Accuracy	Recall	AUC-ROC	NPV	OEI ³	TP	TN	FP	FN	Accuracy	Recall	AUC-ROC	NPV	OEI ³		
Aimbot	F1-Score	448	7,305	392	416	0.906	0.519	0.734	0.946	5,000	548	6,928	1,235	336	0.826	0.620	0.734	0.954	3,000		
	Accuracy	269	7,528	169	595	0.911	0.311	0.645	0.927	5,640	305	7,888	275	579	0.906	0.345	0.656	0.932	5,014		
	AUC-ROC	648	4,603	3,094	216	0.613	0.750	0.674	0.955	1,639	691	4,364	3,799	193	0.559	0.782	0.658	0.958	1,508		
	Acc _{rc} >0.75	652	5,321	2,376	212	0.698	0.755	0.723	0.962	2,052	672	5,365	2,798	212	0.667	0.760	0.709	0.962	1,907		
	Acc _{rc} >0.8	700	4,611	3,086	164	0.620	0.810	0.705	0.966	1,769	716	4,700	3,463	168	0.599	0.810	0.693	0.965	1,693		
	Acc _{rc} >0.85	736	3,790	3,907	128	0.529	0.852	0.672	0.967	1,519	761	3,875	4,288	123	0.512	0.861	0.668	0.969	1,495		
	Acc _{rc} >0.9	778	2,859	4,838	86	0.425	0.900	0.636	0.971	1,333	787	2,955	5,208	97	0.414	0.890	0.626	0.968	1,301		
	F1-Score	576	8,313	432	391	0.915	0.596	0.773	0.955	5,481	651	8,040	1,209	374	0.846	0.635	0.752	0.956	3,352		
	Accuracy	374	8,582	163	593	0.922	0.387	0.684	0.935	6,543	167	9,158	91	858	0.908	0.163	0.577	0.914	5,932		
	Acc _{rc} >0.7	677	7,898	847	290	0.883	0.700	0.802	0.965	4,304	803	7,506	1,743	222	0.809	0.783	0.797	0.971	3,071		
Wallhack	Acc _{rc} >0.75	727	7,589	1,156	240	0.856	0.752	0.810	0.969	3,759	859	6,964	2,285	166	0.761	0.838	0.795	0.977	2,675		
	Acc _{rc} >0.8	776	7,186	1,559	191	0.820	0.802	0.812	0.974	3,251	583	8,280	969	442	0.863	0.569	0.732	0.949	3,574		
	Acc _{rc} >0.85	822	6,712	2,033	145	0.776	0.850	0.809	0.979	2,831	871	6,810	2,439	154	0.748	0.850	0.793	0.978	2,579		
	Acc _{rc} >0.9	871	5,755	2,990	96	0.682	0.901	0.779	0.984	2,229	855	6,885	2,364	170	0.753	0.834	0.789	0.976	2,598		

¹CT: Cheat type; ²Optimizer: Task-Specified Threshold Optimizer in MVIN; ³OEI: Operational Efficiency Index.

catch all cheaters. They sometimes balance catching cheaters with permissiveness, as certain cheaters may bring short-term profits (e.g., in buyout games, where bans may be delayed until after refund periods). When complaints rise, GMs may then conduct a mass ban (a regularly organized operation to clean up the gaming environment) to restore community confidence. This also partially draws to the creation of MVIN.

6.7 Robustness to Cheat Evolution

Although anti-cheat measures are often opaque to prevent circumvention, cheat developers treat them as black boxes, adapting and camouflaging their cheats on a timely basis to evade detection. *Cheat evolution* refers to the diminishing effectiveness of specific anti-cheat over time. Commercially used anti-cheat methods (e.g., signature or process detection, driver scanning, etc.) are susceptible to this evolution since they target specific cheats. However, HAWK starts the analysis from the behavior, thus cheaters should appear data-level dis-

tinctions mentioned in Section 2.2. Hence, no matter how the cheats adapt, as long as the cheaters still want to gain unfair advantages, it is hard to bypass the detection of HAWK. To address **RQ.4**, we test HAWK's robustness to cheat evolution using the *Aimbot* dataset, divided into partitions (40 *matches* each). Classified through date, the dataset is divided into partitions (40 *matches* per partition). The reason for selecting the *Aimbot* dataset is that during its collection window, an official mass ban on aimbots took place (at the 10th partition), and the cheats are usually updated within a few days after such an incident. Figure 7 and Figure 8 demonstrate the ablated performances of subsets under different metrics of HAWK across different numbers of partitions for training. According to the average ban duration of the official manual inspections in Table 4, approximately three sequestration ban cycles have passed during the collection window, and at least two ban cycles after the mass ban occurred. The ablated results of HAWK on both sets have been fluctuating to maintain within a

small range over partitions (time) and with the cheat evolution. Besides, in Figure 6, we observe the effectiveness of HAWK has not continuously decreased over time on both datasets (we separated and extended the collection windows in *Wallhack* dataset for further proof). Thus, both of the results indicate HAWK is robust to cheat evolution.

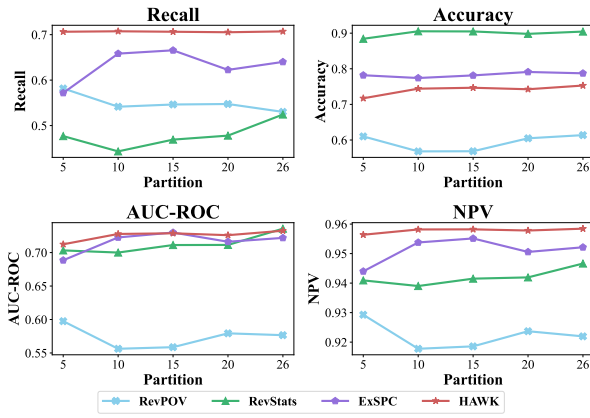


Figure 7: Ablated robustness against cheat evolution over partitions on *Aimbot*'s validation set under different metrics.

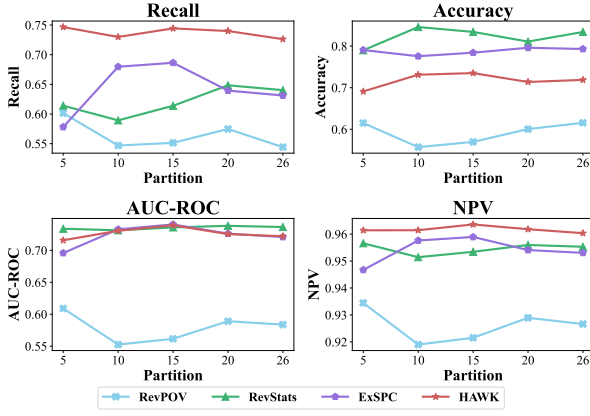


Figure 8: Ablated robustness against cheat evolution over partitions on *Aimbot*'s test set under different metrics.

6.8 Detecting Uncaught Cheaters in the Wild

To answer **RQ.5**, given the above-known presence of cheaters in the false positives in Table 4 after the *first labeling*, we conduct a use case analysis to explore if there are additional illegal activities that exist after the *second labeling*. Given the lengthy average duration of a match, which demands significant manpower, we randomly select 30 HAWK's false positives from the *Aimbot* and *Wallhack* validation sets for manual review, respectively (experts' skill level is listed in Table 8).

With the assistance of three experts in FPS games, we identify 27 suspects, who are labeled as *normal players* after the second labeling, to be highly suspicious within these 60 false positives. Of these 27 suspects, 14 originate from the *Aimbot* dataset (4 are considered using *aimbots* and 10 are considered *boosting*, i.e., elevate the account rank by other higher-rank players playing the account), while 13 are from the *Wallhack* dataset (8 are considered using *wallhacks* and 5 are considered *boosting*). We reported these suspicions to the official personnel. Upon their review, they confirm all 12 of the aforementioned *aimbots* and *wallhacks* suspects are committed to cheats, subsequently issuing bans for these cheaters on the platform. This reaffirms the poor performance of current in-use anti-cheats and the datasets used for training and evaluation are not entirely pristine. The website mentioned in Section 1 demonstrates their illegal actions. In terms of *boosting* suspects, there are no existing solutions for the officials to evidently verify their illegal actions. Therefore, there are no bans issued on the suspicious *boosting* accounts.

Table 7: Maximum overheads of HAWK's subsystems per match. The numbers are retrieved by the Time [36] in Linux.

Max. Overheads per Match	REVPOV	REVSTATS	EXSPC	MVIN
User time (sec) ¹	415.72	178.12	36.89	3.97
System time (sec) ²	69.32	436.61	27.12	13.53
Elapsed time (mm:ss) ³	03:40	00:14	00:45	00:01
Percent of CPU this job got ⁴	220%	4371%	140%	2860%
Maximum resident set size (GB) ⁵	3.56	0.27	2.57	0.10

¹**User time:** CPU time spent in user mode;

²**System time:** CPU time spent in the kernel or system mode;

³**Elapsed time:** Total real-world time taken to execute the job;

⁴**Percent of CPU this job got:** How much of the available CPU resources were allocated to the process, this value is commonly greater than 100% when the process runs on multiple CPU cores;

⁵**Maximum resident set size:** The peak amount of physical memory that the process used.

6.9 HAWK's Overheads

HAWK is developed as an asynchronous, load-balancing system that analyzes post-game *replay files* during periods of low server activity. It operates independently of active game servers and can be deployed on a separate server. However, we still conduct overhead assessments for reference. To answer **RQ.6**, we utilize an Ubuntu server equipped with 128 cores AMD EPYC 7713P 64-Core Processor and 256 GB RAM to mimic a real dedicated game server [19]. By leveraging the pre-trained model in the artifact, HAWK requires only CPU computing resources to function gracefully. Table 7 indicates the maximum overhead statistics per match, with each match analyzed concurrently. In addition to the basic overheads, we also estimate the HAWK-to-server overheads in terms of a real deployment scenario. Our platform partner reports that at most 150,000 matches are played daily. Each server needs to run at most 573 matches a day. According to our platform's

report and the public server statistics [56], player activity is at its lowest, typically 1-5 AM local time. During this timeframe, at most 144 matches need to be analyzed per hour. Thus, according to the elapsed time mentioned in Table 7, at most it needs to process 12 matches concurrently to finish processing all matches within the timeframe per server. We further conduct concurrent processing evaluation, it occupies at most 17.95% memory and 35.45% CPU usage for processing 12 matches concurrently. Therefore, each server possesses more than sufficient resources for deploying HAWK, even if several matches are hosted at the same time.

7 Discussions

Generalizability. Narrowed generalizability is a meta-problem for the anti-cheat field. Since the cheat is game-specified, the anti-cheat is hard to generalize for all games. Although we successfully implemented HAWK on one of the leading tactical shooter games [64] (a subgenre of FPS games like CS:GO), like other prior works [2, 9, 24, 39, 69, 70] discussed in Section 8, it requires further adaptation for other FPS subgenres with distinct gameplay. HAWK’s generalizability concerns on the core observations, methodologies, and workflow rather than specific features. The features presented are theoretically applicable to tactical shooters in FPS games like the CS series, CrossFire, and others. However, adaptation is needed for other subgenres, where certain elements like flashes and grenades may not apply. For instance, Hero Shooters (e.g., Overwatch, Valorant) where such features could be substituted with character-specific abilities, or Battle Royale (BR) games (e.g., Fortnite, PUBG) where elements like angles and velocities need substitution due to long time-to-kill. Since the *replay files* and labelings are significant for HAWK, also due to the dataset scarcity limitation, conducting further research on different subgenres to prove the generalizability of HAWK must require cooperation with the game vendors to obtain the data. We have initiated contact with several vendors, and one specializing in BR games has shown interest in cooperating. But, we have to leave specific implementation and evaluation for future work.

Manual involvement. Although HAWK has significantly increased the detection performance and efficiency, as mentioned in Section 3.2, HAWK-after-use manual verification is unavoidable. The presence of real false positives undeniably indicates the requirement for manual checks to avoid false bans. Nevertheless, with the mitigation of the limitations mentioned in Section 1, we still believe HAWK plays an important role in the FPS games’ server-side anti-cheat.

8 Related Works

Client-side detection. BotScreen [9], as the latest *aimbot* detector, utilizes TEE (Intel SGX) to store and run the de-

tection model with aiming features. It leverages a self-setup server and hires 14 players to play in Deathmatch instead of the rank mode. Thus, BotScreen is limited to dataset scarcity, and its real-world functionality remains unclear, especially with more complex scenarios. BotScreen evaluates with a basic, open-source *aimbot* Osiris [37], which is game-specific and may not reflect the performance against more sophisticated cheats [42, 44]. VAC [12] can detect *wallhack* by using OpenGL and scanning such as DNS cache to verify if the suspect has purchased and cheated in a game for Counter-Strike [12, 38]. Warden [61] scans the system running programs, users’ browser history, and cookies to determine a user’s behavior for Blizzard’s games. EAC [22], BattlEye [3], and XIGNCODE3 [62] are commercial anti-cheats. They can achieve both cheat detection and prevention [53] for multiple platforms and different games after customization by monitoring and managing process privileges. Vanguard [30] is a kernel-level anti-cheat for VALORANT [51] that has full access and control over the system. The above client-side anti-cheats are limited to hardware constraints, security and privacy concerns, and client overheads. And reflect the limited generalizability problem for anti-cheat.

Client-side prevention. BlackMirror [49] applies SGX for anti-wallhack, providing the client GPU only visible entities based on local predictions. It only prevents without detecting and is limited to hardware constraints, client overheads, and targeting on a specific cheat type or subcategories. Invisibility Cloak [58] prevents *computer-vision-based aimbots* from performing object detection with the screen images but is ineffective against memory-based *aimbots* and *wallhacks*.

Server-side ML-based detection. Yeung et al. [69] initially proposed a Bayesian model to tune the probability threshold with basic statistics in 2006, but it is outdated for today’s advanced cheating techniques. Subsequent works [2, 24, 39, 70] used machine learning with basic statistics or limited features, which couldn’t monitor sophisticated behaviors or describe entire matches [9]. These earlier works are limited to naive features and workflow, unclear performance, and dataset scarcity. They require extra modification (specified to the game) on the game engine to collect and construct features in parallel with the game commencing. Therefore, it is also hard to generalize their method to other games.

9 Conclusion

We proposed an FPS games’ server-side anti-cheat framework HAWK, drawing inspiration from how humans identify cheaters. With promising experimental results, we have demonstrated HAWK’s real-world effectiveness, efficiency, and robustness in identifying cheaters in a modern FPS game. Ultimately, we hope HAWK can be a pathfinder for next-generation FPS anti-cheat, providing a valuable dataset and a reference for the follow-up research.

10 Ethics Considerations

The dataset only contains information including in-game operations and data, avatars' IDs, and the banning information, which are all publicly accessible⁴. We will anonymize all information that may disclose the player's privacy, i.e., the player ID. The information in the published dataset will not directly or indirectly cause any form of impact or damage to the game and/or to its distributors, and/or to the players and/or the community. The data provider approves the release and reuse of the dataset for research purposes. No private information will be disclosed through our dataset. The studies were conducted in accordance with the local legislation and institutional requirements.

11 Compliance to Open Science Policy

We open-source HAWK and our datasets⁵ to support open science. We will make all links publicly available after paper acceptance. Artifacts will be submitted to the Artifact Evaluation Committee for further review.

References

- [1] AFK Gaming. 8 types of hacks and cheats in CS:GO. <https://afkgaming.com/csgo/news/2619-8-types-of-hacks-and-cheats-in-csgo>, 2019.
- [2] Hashem Alayed, Fotos Frangoudes, and Clifford Neuman. Behavioral-based cheating detection in online first person shooters using machine learning techniques. In *2013 IEEE Conference on Computational Intelligence in Games (CIG)*, pages 1–8, Niagara Falls, ON, Canada, Aug 2013. IEEE.
- [3] BattlEye Innovations. Interested in using BattlEye? <https://www.battleye.com/>, 2024.
- [4] Zhanna Belyaeva, Anait Petrosyan, and Riad Shams. Stakeholder data analysis in the video gaming industry: Implications for regional development. *EuroMed Journal of Business*, 17, 05 2022.
- [5] BleepingComputer. New intel chips won't play blu-ray disks due to sgx deprecation. <https://www.bleepingcomputer.com/news/security/new-intel-chips-wont-play-blu-ray-disks-due-to-sgx-deprecation/>, 2022. Accessed: 2024-02-27.
- [6] Leo Breiman. Bagging predictors. *Machine Learning*, 24(2):123–140, 1996.
- [7] Leo Breiman. Random forests. *Machine learning*, 45:5–32, 2001.
- [8] bright, IDontCode, irql0. EasyAntiCheat Exploit to inject unsigned code into protected processes. <https://blog.back.engineering/10/08/2021/>, August 2021. Accessed: 2024-02-29.
- [9] Minyeop Choi, Gihyuk Ko, and Sang Kil Cha. Botscreen: trust everybody, but cut the aimbots yourself. In *Proceedings of the 32nd USENIX Conference on Security Symposium, SEC '23, USA, 2023*. USENIX Association.
- [10] William W. Cohen. Fast effective rule induction. In *Proceedings of the Twelfth International Conference on International Conference on Machine Learning, ICML'95*, page 115–123, San Francisco, CA, USA, 1995. Morgan Kaufmann Publishers Inc.
- [11] Mia Consalvo. *Cheating: Gaining Advantage in Videogames*. MIT Press, Cambridge, MA, 2007.
- [12] Valve Corporation. Valve anti-cheat (vac) system. https://help.steampowered.com/en/faqs/view/571_A-97DA-70E9-FF74, 2023.
- [13] Corinna Cortes and Vladimir Vapnik. Support-vector networks. *Machine learning*, 20:273–297, 1995.
- [14] Jan Salomon Cramer. The origins of logistic regression. Tinbergen Institute Discussion Papers 02-119/4, Tinbergen Institute, 2002.
- [15] CVE-2019-16098. CVE-2019-16098: Vulnerability in MSI Afterburner. <https://nvd.nist.gov/vuln/detail/CVE-2019-16098>, 2019. Accessed: 2023-12-07.
- [16] CVE-2020-36603. CVE-2020-36603: Vulnerability in Genshin Impact Anti-Cheat Software. <https://nvd.nist.gov/vuln/detail/CVE-2020-36603>, 2022. Accessed: 2023-12-07.
- [17] CVE-2021-3437. CVE-2021-3437: HP OMEN Gaming Hub Privilege Escalation Bug Hits Millions of Gaming Devices. <https://www.sentinelone.com/labs/cve-2021-3437-hp-omen-gaming-hub-privilege-escalation-bug-hits-millions-of-gaming-devices/>, 2021. Accessed: 2023-12-07.
- [18] CVE-2023-38817. CVE-2023-38817: Vulnerability in Minecraft Anti-Cheat Tool. <https://nvd.nist.gov/vuln/detail/CVE-2023-38817>, 2023. Accessed: 2023-12-07.
- [19] DatHost. CS2 Server Hosting. <https://dathost.net/cs2-server-hosting>, 2024. Accessed: 2024-06-05.

⁴Link. We anonymize the platform's URL and name.

⁵Link. The repository and dataset will be released upon acceptance. Artifacts are uploaded for the reference. Ethics statement is shown in Section 10.

[20] Gülşen Demiröz and H Altay Güvenir. Classification by voting feature intervals. In *European Conference on Machine Learning*, pages 85–92, Berlin, Heidelberg, 1997. Springer.

[21] Tapani Elomaa and Matti Kaariainen. An analysis of reduced error pruning. *Journal of Artificial Intelligence Research*, 15:163–187, 2001.

[22] Epic Games, Inc. Easy Anti-Cheat. <https://www.easy.ac/>, 2024.

[23] Shufan Fei, Zheng Yan, Wenxiu Ding, and Haomeng Xie. Security vulnerabilities of sgx and countermeasures: A survey. *ACM Comput. Surv.*, 54(6), jul 2021.

[24] Luca Galli, Daniele Loiacono, Luigi Cardamone, and Pier Luca Lanzi. A cheating detection framework for unreal tournament iii: A machine learning approach. In *2011 IEEE Conference on Computational Intelligence and Games (CIG'11)*, pages 266–272, Seoul, Korea (South), 2011. IEEE.

[25] Steven Gianvecchio, Zhenyu Wu, Mengjun Xie, and Haining Wang. Battle of botcraft: fighting bots in online games with human observational proofs. In *Proceedings of the 16th ACM Conference on Computer and Communications Security, CCS '09*, page 256–268, New York, NY, USA, 2009. Association for Computing Machinery.

[26] Grzegorz Góra and Arkadiusz Wojna. Riona: A classifier combining rule induction and k-nn method with automated selection of optimal neighbourhood. In *Machine Learning: ECML 2002: 13th European Conference on Machine Learning Helsinki, Finland, August 19–23, 2002 Proceedings 13*, pages 111–123, Berlin, Heidelberg, 2002. Springer.

[27] Mee Lan Han, Jung Kyu Park, and Huy Kang Kim. Online game bot detection in fps game. In *Proceedings of the 18th Asia Pacific Symposium on Intelligent and Evolutionary Systems-Volume 2*, pages 479–491. Springer, 2015.

[28] Simon Haykin. *Neural networks: a comprehensive foundation*. Prentice Hall PTR, USA, 1994.

[29] Sepp Hochreiter and Jürgen Schmidhuber. Long short-term memory. *Neural Computation*, 9(8):1735–1780, 1997.

[30] Riot Games Inc. What is vanguard? <https://support.valorant.riotgames.com/hc/en-us/articles/360046160933-What-is-Vanguard->, Jun 2022.

[31] Intel Community. Rising to the challenge: Data security with intel confidential. <https://community.intel.com/t5/Blogs/Products-and-Solutions/Security/Rising-to-the-Challenge-Data-Security-with-Intel-Confidential/post/1353141>, 2022. Accessed: 2024-02-27.

[32] Irdeto. Cheating in video games: The A to Z. <https://blog.irdeto.com/video-gaming/cheating-in-games-everything-you-always-wanted-to-know-about-it/>, 2023.

[33] JARVIS THE NPC. Warzone Reddit Outcry: Anti-Cheat Failures Fuel Frustration Among Players. <https://www.zleague.ggg/theportal/warzone-reddit-outcry-anti-cheat-failures-fuel-frustration-a-mong-players/>, April 2024. Accessed: 2024-04-24.

[34] George H. John and Pat Langley. Estimating continuous distributions in bayesian classifiers. In *Proceedings of the Eleventh Conference on Uncertainty in Artificial Intelligence, UAI'95*, page 338–345, San Francisco, CA, USA, 1995. Morgan Kaufmann Publishers Inc.

[35] Anssi Kanervisto, Tomi Kinnunen, and Ville Hautamäki. Gan-aimbots: Using machine learning for cheating in first person shooters. *IEEE Transactions on Games*, 15(4):566–579, 2023.

[36] Michael Kerrisk. time(1) — Linux manual page. <https://man7.org/linux/man-pages/man1/time.1.htm>, 1, 2024. Accessed: 2024-06-05.

[37] Daniel Krupiński. Osiris. <https://github.com/danielkrupinski/Osiris>, 2023. Accessed: 2024-02-27.

[38] Samuli Lehtonen et al. Comparative study of anti-cheat methods in video games. *University of Helsinki, Faculty of Science*, 2020.

[39] Daiping Liu, Xing Gao, Mingwei Zhang, Haining Wang, and Angelos Stavrou. Detecting passive cheats in online games via performance-skillfulness inconsistency. In *2017 47th Annual IEEE/IFIP International Conference on Dependable Systems and Networks (DSN)*, pages 615–626, Denver, CO, USA, 2017. IEEE.

[40] Shengmei Liu, Mark Claypool, Atsuo Kuwahara, Jamie Sherman, and James J Scovell. Lower is better? the effects of local latencies on competitive first-person shooter game players. In *Proceedings of the 2021 CHI Conference on Human Factors in Computing Systems, CHI '21*, New York, NY, USA, 2021. Association for Computing Machinery.

[41] Minh-Thang Luong, Hieu Pham, and Christopher D. Manning. Effective approaches to attention-based neural machine translation, 2015.

[42] m2qchqo110. The Most Hilarious Complaints We've Heard About PUBG Aimbot. <https://medium.com/@m2qchqo110/the-most-hilarious-complaints-weve-heard-about-pubg-aimbot-13a2a2a2a2a2>

p5hvlpr124/the-most-hilarious-complaints-weve-heard-about-pubg-aimbot-b596bbcb1ce5, August 2019. Accessed: 2024-06-13.

[43] Anton Maario, Vinod Kumar Shukla, A. Ambikapathy, and Purushottam Sharma. Redefining the risks of kernel-level anti-cheat in online gaming. In *2021 8th International Conference on Signal Processing and Integrated Networks (SPIN)*, pages 676–680, Noida, India, 2021. IEEE.

[44] Mike Scorpio. What You Should Know About Aimbots Before Using Them in a Video Game. <https://miketendo64.com/2021/01/07/what-you-should-know-about-aimbots-before-using-them-in-a-video-game/>, January 2021. Accessed: 2024-06-13.

[45] Kevin Kjelgren Mikkelsen. Information security as a countermeasure against cheating in video games. Master's thesis, NTNU, 2017.

[46] Kevin P Murphy et al. Naive bayes classifiers. *University of British Columbia*, 18(60):1–8, 2006.

[47] Newzoo. Newzoo global games market report 2021 | free version. <https://newzoo.com/resources/trend-reports/newzoo-global-games-market-report-2021-free-version>, July 2021.

[48] Newzoo. Newzoo's global games market report 2023 | january 2024 update. <https://newzoo.com/resources/trend-reports/newzoo-global-games-market-report-2023-free-version>, Febuary 2024.

[49] Seonghyun Park, Adil Ahmad, and Byoungyoung Lee. Blackmirror: Preventing wallhacks in 3d online fps games. In *Proceedings of the 2020 ACM SIGSAC Conference on Computer and Communications Security*, CCS '20, page 987–1000, New York, NY, USA, 2020. Association for Computing Machinery.

[50] RYAN K. RIGNEY. The gamers do not understand anti-cheat. <https://www.pushtotalk.gg/p/the-gamers-do-not-understand-anti-cheat>, Febuary 2024. Accessed: 2024-04-24.

[51] Riot Games. Valorant official website. <https://playvalorant.com/>. Accessed: 2024-08-31.

[52] Michael J Siers and Md Zahidul Islam. Software defect prediction using a cost sensitive decision forest and voting, and a potential solution to the class imbalance problem. *Information Systems*, 51:62–71, 2015.

[53] José Nuno Silva. Towards automated server-side video game cheat detection. <https://repositorio-aberto.up.pt/bitstream/10216/142935/2/572983.pdf>, July 2022.

[54] Nitish Srivastava, Geoffrey Hinton, Alex Krizhevsky, Ilya Sutskever, and Ruslan Salakhutdinov. Dropout: A simple way to prevent neural networks from overfitting. *J. Mach. Learn. Res.*, 15(1):1929–1958, jan 2014.

[55] Santosh Srivastava, Maya R. Gupta, and Béla A. Frigyik. Bayesian quadratic discriminant analysis. *Journal of Machine Learning Research*, 8(46):1277–1305, 2007.

[56] SteamDB. Counter-Strike 2 Steam Charts. <https://steamdb.info/app/730/charts/#48h>, 2024. Accessed: 2024-06-05.

[57] Jerzy Stefanowski. *On Combined Classifiers, Rule Induction and Rough Sets*, pages 329–350. Springer, Berlin, Heidelberg, 2007.

[58] Chenxin Sun, Kai Ye, Liangcai Su, Jiayi Zhang, and Chenxiong Qian. Invisibility cloak: Proactive defense against visual game cheating. In *33rd USENIX Security Symposium (USENIX Security 24)*, pages 3045–3061, Philadelphia, PA, August 2024. USENIX Association.

[59] Bill Toulias. Apex Legends players worried about RCE flaw after ALGS hacks. <https://www.bleepingcomputer.com/news/security/apex-legends-players-worried-about-rce-flaw-after-algs-hacks/>, March 2024. Accessed: 2024-04-08.

[60] Tracker Network. Tracker Network: Find your stats for your favorite games. <https://tracker.gg/>, 2024. Accessed: 2024-04-28.

[61] Mark Ward. Technology | warcraft game maker in spying row. <http://news.bbc.co.uk/2/hi/technology/4385050.stm>, Oct 2005.

[62] LTD WELLBIA.COM CO. Wellbia. <https://wellbia.com/>, 2023.

[63] WePC. Video Game Industry Statistics, Trends and Data In 2023. <https://www.wepc.com/news/video-game-statistics/>, 2023.

[64] Wikipedia. Tactical shooter. https://en.wikipedia.org/wiki/Tactical_shooter, 2024. Accessed: 2024-06-14.

[65] Leland Wilkinson, Anushka Anand, and Dang Nhon Tuan. Chirp: a new classifier based on composite hypercubes on iterated random projections. In *Proceedings of the 17th ACM SIGKDD International Conference on Knowledge Discovery and Data Mining*, KDD '11, page 6–14, New York, NY, USA, 2011. Association for Computing Machinery.

[66] Tim Witschel and Christian Wressnegger. Aim low, shoot high: Evading aimbot detectors by mimicking

user behavior. In *Proceedings of the 13th European Workshop on Systems Security, EuroSec ’20*, page 19–24, New York, NY, USA, 2020. Association for Computing Machinery.

[67] Peter Xenopoulos. awpy: A Python package for Counter-Strike: Global Offensive data parsing, analytics, and visualization. <https://pypi.org/project/awpy/>, 2023. Accessed: 2023-12-07.

[68] Darren Yates, Md Zahidul Islam, and Junbin Gao. Spaarc: a fast decision tree algorithm. In *Data Mining: 16th Australasian Conference, AusDM 2018, Bahrurst, NSW, Australia, November 28–30, 2018, Revised Selected Papers 16*, pages 43–55, Singapore, 2019. Springer.

[69] S.F. Yeung, J.C.S. Lui, Jiangchuan Liu, and J. Yan. Detecting cheaters for multiplayer games: theory, design and implementation[1]. In *CCNC 2006. 2006 3rd IEEE Consumer Communications and Networking Conference, 2006.*, volume 2, pages 1178–1182, Las Vegas, NV, USA, 2006. IEEE.

[70] Su-Yang Yu, Nils Hammerla, Jeff Yan, and Peter Andras. A statistical aimbot detection method for online fps games. In *The 2012 International Joint Conference on Neural Networks (IJCNN)*, pages 1–8, Brisbane, QLD, Australia, 2012. IEEE.

[71] Nan Zheng, Aaron Paloski, and Haining Wang. An efficient user verification system using angle-based mouse movement biometrics. *ACM Transactions on Information and System Security (TISSEC)*, 18(3):1–27, 2016.

Table 8: Experts’ skill level for sampled match review, all stats are retrieved from [60].

Expert	Playtime	Skill Level
#1	>7,000hrs	CS:GO - Premier 19,000 (Top 2.62%) Overwatch2 - Role Grand Master (Top 1.46%) Apex Legend - BR Master (Top 0.6%)
#2	>1,400hrs	CS:GO - Premier 19,200 (Top 2.62%)
#3	>5,000hrs	CS:GO - Premier 18,000 (Top 4.59%)

A Training and Validation Loss for ExSPC Model

The training process on each of the datasets in ExSPC utilizes the validation set for optimization. Figure 9 and Figure 10 demonstrate the training and validation loss for each dataset respectively. It is noticeable that the individual results are not ideal. Thus, we use the multi-view design to complement one another of the subsystems.

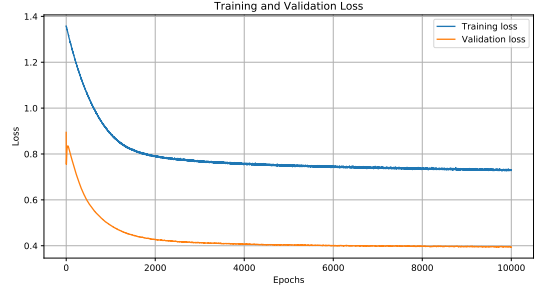


Figure 9: Training and validation loss of ExSPC on *Wallhack* dataset.

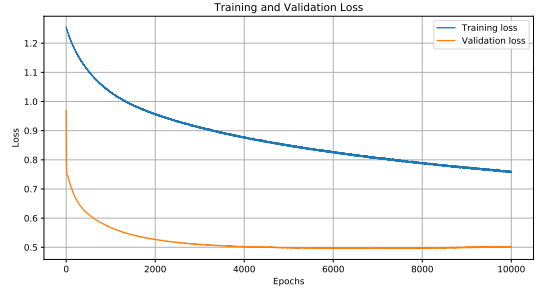


Figure 10: Training and validation loss of ExSPC on *Aimbot* dataset.

B Temporal Features

B.1 Engagement features

Engagement features are extracted at each tick of the event occurrence. The introduction of the Engagement features is as follows:

- **Damage features:**
 - **tick:** the tick number;
 - **seconds:** the time elapsed within a round in second;
 - **attackerSteamID, victimSteamID:** the ID of the player;
 - **attackerSide, victimSide:** the team side of the player;
 - **attackerX, attackerY, attackerZ, victimX, victimY, victimZ:** the X, Y, and Z location coordination in \mathbb{R}^3 of the player;
 - **attackerViewX, attackerViewY, victimViewX, victimViewY:** the X and Y view direction coordination in \mathbb{R}^2 of the player;
 - **attackerStrafe:** the Boolean value indicates whether the attacker is moving sideways relative to their forward direction;
 - **weapon:** the ID of the damage-caused weapon;
 - **weaponClass:** the class ID of the damage-caused

- **weapon**;
- **hpDamage**: the value of damage caused to the victim;
- **hpDamageTaken**: the value of damage taken by the victim;
- **armorDamage**: the value of the damage caused to the victim’s armor;
- **armorDamageTaken**: the value of damage taken by the victim’s armor;
- **hitGroup**: the ID of the damage-taken area on the body of the victim;
- **isFriendlyFire**: the Boolean value indicates whether the damage is from the friendly;
- **distance**: the distance between the attacker and the victim;
- **zoomLevel**: the zoom level of the attacker’s weapon;
- **roundNum**: the round number of the current tick.
- **Auxiliary props features**: The tick, second, IDs, sides, location, view direction, and round number are similar to above;
 - **flashDuration**: the time elapsed for the blinding effect affects on the victim in second;
- **Offensive props features**: The ID, side, location, view direction of the thrower and the prop, and round number are similar to above;
 - **throwTick, destroyTick**: the tick of the prop thrown or destroyed;
 - **throwSeconds, destroySeconds**: the time elapsed within a round in seconds at the moment of the prop thrown or destroyed;
- **Elimination features**: The tick, second, IDs, sides, location, view direction, distance, weapon, weapon class, and round number are similar as above;
 - **assisterSteamID**: the ID of the assister;
 - **assisterSide**: the team side of the assister;
 - **isSuicide**: the Boolean value indicates whether the elimination is a suicide event;
 - **isTeamkill**: the Boolean value indicates whether the elimination is a team kill event;
 - **isWallbang**: the Boolean value indicates whether the elimination is conducted by occluder penetration;
 - **penetratedObjects**: the number of obstacles the bullet penetrated;
 - **isFirstKill**: the Boolean value indicates whether the elimination is the first kill within a round;
 - **isHeadshot**: the Boolean value indicates whether the elimination is a head-shot event;
 - **victimBlinded**: the Boolean value indicates whether the victim is blinded;

- **attackerBlinded**: the Boolean value indicates whether the attacker is blinded;
- **flashThrowerSteamID**: the ID of the flash-thrower;
- **flashThrowerSide**: the team side of the flash-thrower;
- **noScope**: the Boolean value indicates whether the elimination is conducted with no scoped;
- **thruSmoke**: the Boolean value indicates whether the elimination is conducted through smoke;
- **isTrade**: the Boolean value indicates whether the elimination is traded with the opponent;
- **Weapon fire features**: The IDs, sides, location, view direction, weapon, weapon class, player strafe, zoom level of the attacker, and the tick, second, and round number are similar as above;
 - **ammoInMagazine**: the number of ammunition in the magazine;
 - **ammoInReserve**: the number of ammunition in the reserve;

B.2 Movement features

Movement features are extracted per tick. The IDs, sides, location, view direction of the player, and the tick, second, and round numbers are similar to those above. The rest of the introduction of the Movement features is as follows:

- **velocityX, velocityY, velocityZ**: the velocity of the player in 3D space;
- **isAlive**: the Boolean value indicates whether the player is alive;
- **isBlinded**: the Boolean value indicates whether the player is blinded;
- **isAirborne**: the Boolean value indicates whether the player is feet dangling;
- **isDucking**: the Boolean value indicates whether the player is ducking;
- **isDuckingInProgress**: the Boolean value indicates whether the player is ducking in progress;
- **isUnDuckingInProgress**: the Boolean value indicates whether the player is standing up from ducking in progress;
- **isDefusing**: the Boolean value indicates whether the player is defusing the bomb;
- **isPlanting**: the Boolean value indicates whether the player is planting the bomb;
- **isReloading**: the Boolean value indicates whether the player is reloading;
- **isInBombZone**: the Boolean value indicates whether the player is in the bomb planting area;
- **isStanding**: the Boolean value indicates whether the player is standing;

- **isScoped**: the Boolean value indicates whether the player is scoped with the weapon;
- **isWalking**: the Boolean value indicates whether the player is walking;
- **IsolationDegree**: the distance to the calculation center of each teammate.

B.3 Economy features

Economy features are extracted per round. The introduction of the Economy features are as follows:

- **round**: the number of round;
- **equipmentValueFreezetimeEnd**: the value of the player’s equipment after the end of the freeze time (the interval from the commencement of a round to the moment players are granted the ability to move and fire. This period typically allows players to purchase equipment);
- **equipmentValueRoundStart**: the value of the player’s equipment at the start of each round;
- **cash**: the amount of money the player obtains at the end of each round;
- **cashSpendTotal**: the amount of money the player spends within each round.

C Structured Features

In this section, the extracted data from demos are further processed to create strong-expressiveness features that can indicate the sense and performance of a player clearly. For notations used in the formulas throughout this section, please refer to [Table 9](#).

C.1 Aiming features

Durations [Figure 11](#) illustrates the three distinct moments that form three different durations. In terms of the moments, t_0 denotes the moment that the current player initially spots one opponent. In [Figure 11](#), a1 and a2 present a possible set of states at t_0 . In which a1 represents a 3-dimensional world in the game map, where the opponent happens to appear at the edge of the current player’s field of view (FOV). And a2 demonstrates the 2-dimensional state correspondingly which is typically displayed through the player’s monitor, where the opponent also happens to be spotted at the edge of the current player’s POV. t_1 denotes the moment that the current player notices the hostile movement and initiates responsive action (*i.e.*, open fire). Note that at t_1 the current firing event may or may not be equivalent to a damage event upon the opponent. t_2 denotes the moment that the current player performs a damage event upon the opponent within one period of valid engagement for the first time. In our case, the threshold for

resetting the valid engagement period detection (*i.e.*, no opponent in sight, no damage or firing event) is set as 10 seconds. In [Figure 11](#), it demonstrates a series of generic circumstances that often happen in games where the positions of the current player and the opponent vary along from t_0 to t_2 . And it is common that sometimes t_1 and t_2 are overlapped. In terms of durations, the elapsed period from t_0 to t_1 is defined as *reaction time* (*rat*). The elapsed period from t_1 to t_2 is defined as *adjustment time* (*ajt*). The elapsed period from t_0 to t_2 is defined as *duration time* (*drt*). The average and variance calculations are applied after obtaining the data. The average performance of all samples is obtained through the average, and the degree of dispersion of the samples is represented by the variance. The integration of average and variance is able to represent the overall performance and stability of the current player within a match.

rat average. Denotes the average performance regarding *rat* of the current player among one match. The lower this feature is, the faster the player reacts.

$$\mathbf{F}_{\text{rat-avg}}(\mathbf{i}) = \overline{RAT} = \frac{\sum_{j=1}^N RAT_j}{N} \quad (11)$$

where N denotes $\#(RAT)$ within a match.

rat variance. Denotes the degree of dispersion of *rat* distributions of the current player among one match.

$$\mathbf{F}_{\text{rat-var}}(\mathbf{i}) = Var(RAT) = \frac{\sum_{j=1}^N (RAT_j - \overline{RAT})^2}{N} \quad (12)$$

where N denotes $\#(RAT)$ within a match.

ajt average. Denotes the average performance regarding *ajt* of the current player among one match. The lower this feature is, the faster the player adjusts.

$$\mathbf{F}_{\text{ajt-avg}}(\mathbf{i}) = \overline{AJT} = \frac{\sum_{j=1}^N AJT_j}{N} \quad (13)$$

where N denotes $\#(AJT)$ within a match.

ajt variance. Denotes the degree of dispersion of *ajt* distributions of the current player among one match.

$$\mathbf{F}_{\text{ajt-var}}(\mathbf{i}) = Var(AJT) = \frac{\sum_{j=1}^N (AJT_j - \overline{AJT})^2}{N} \quad (14)$$

where N denotes $\#(AJT)$ within a match.

Table 9: Notations and descriptions of structured features.

Notation	Description	Notation	Description
i	the current player	$E_x^{a \rightarrow b}[k]$	the k^{th} type x event conducted by player a to b
p, p^*	a particular player, any player	$\#(\bullet)$	the number of counts of the parameter
o, o^*	a particular opponent, any opponent	$wp(\bullet)$	the weapon used by a player
a, a^*	a particular ally, any ally	$hg(\bullet)$	the body part hit by a player
ts	through smoke	$t(\bullet)$	the moment of the event occurs in second
$p(\bullet)$	the number of occluders penetrated	$mag(\bullet)$	the number of bullets remain in a player's magazine
$\Delta(\bullet)$	the change in the parameter	$dist(x, y)$	the distance range between entities x and y
$ELAPSE(\bullet)$	the duration from the start to the end of an event	$HEG(\bullet)$	high-explosive grenade is applied by a player
$INC(\bullet)$	incendiary or Molotov is applied by a player	$SMK(\bullet)$	smoke grenade is applied by a player
$FLS(\bullet)$	flash grenade is applied by a player	$FK(\bullet)$	first kill is accomplished by a player

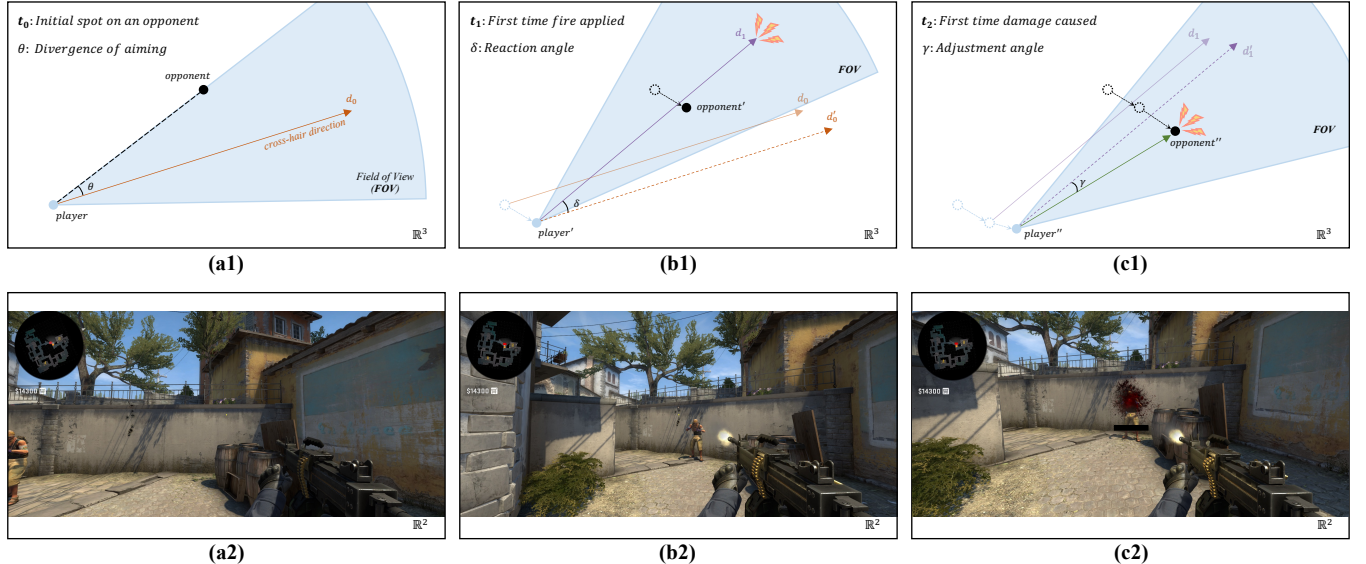


Figure 11: Illustrations of reaction and adjustment features. The black rectangle overlay in c2 hides the player's ID.

drt average. Denotes the average performance regarding *drt* of the current player among one match. The lower this feature is, the faster the player hits.

$$\mathbf{F}_{\text{drt-avg}}(\mathbf{i}) = \overline{DRT} = \frac{\sum_{j=1}^N DRT_j}{N} \quad (15)$$

drt variance. Denotes the degree of dispersion of *drt* distributions of the current player among one match.

$$\mathbf{F}_{\text{drt-var}}(\mathbf{i}) = \text{Var}(DRT) = \frac{\sum_{j=1}^N (DRT_j - \overline{DRT})^2}{N} \quad (16)$$

where N denotes $\#(DRT)$ occurrences within a match.

Velocity *velocity average.* Denotes the average mouse velocity of the current player among one match between t_0 and

t_2 , through which way two features of distance and time period can be highly compressed into one feature. The higher the feature is, the faster the player hits the targets.

$$V = \frac{dist(i, o)}{DRT_i} \quad (17)$$

where o denotes the victim in the specified *DRT*.

$$\mathbf{F}_{\text{v-avg}}(\mathbf{i}) = \overline{V} = \frac{\sum_{j=1}^N V_j}{N} \quad (18)$$

where N denotes $\#(DRT)$ within a match.

velocity variance. Denotes the degree of dispersion of *velocity* distributions of the current player among one match.

$$\mathbf{F}_{\text{v-var}}(\mathbf{i}) = \text{Var}(V) = \frac{\sum_{j=1}^N (V_j - \overline{V})^2}{N} \quad (19)$$

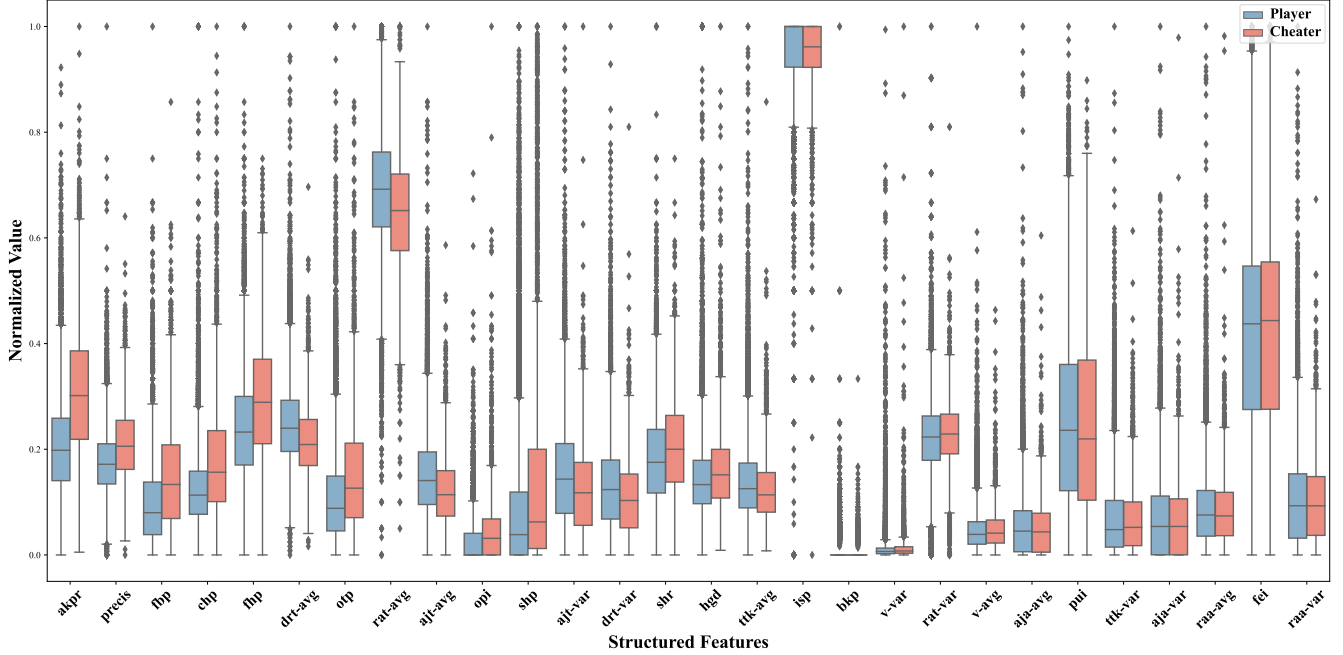


Figure 12: Complete box plots of comparative visualization between honest players and cheaters on all structured features under Mann-Whitney U (Wilcoxon Rank-Sum) test with P-Value ascending (distinction descending) order.

where N denotes $\#(DRT)$ within a match.

Angles Figure 11 illustrates the three different angles, in which θ denotes *divergence of aiming* is extracted by Liu et al. [39] and represents the initial angular divergence between the aiming position and the opponent position. However, the time complexity for obtaining such a feature is too expensive to be accepted for industrial implementation. Therefore we extracted the following features which not only preserve strong expressiveness but also significantly reduce the time cost, as well as innovatively segment each engagement process into three stages. δ represents the *reaction angle (raa)*, which reflects the angle of two cross-hair directions at t_0 and t_1 respectively. γ represents the *adjustment angle (aja)*, which, similarly reflects the angle of two cross-hair directions at t_1 and t_2 respectively. The larger δ and γ are the longer distance the cross-hair travels, which ultimately results in performance divergence. Similarly, the average and variance operation is applied accordingly.

raa average. Denotes the average performance regarding *raa* of the current player among one match. The lower the feature is, the smaller the angle and the less effort the player aims for and puts into reaching their targets.

$$\mathbf{F}_{\text{raa-avg}}(\mathbf{i}) = \overline{RAA} = \frac{\sum_{j=1}^N RAA_j}{N} \quad (20)$$

where N denotes $\#(RAA)$ within a match.

raa variance. Denotes the degree of dispersion of *raa* distributions of the current player among one match.

$$\mathbf{F}_{\text{raa-var}}(\mathbf{i}) = \text{Var}(RAA) = \frac{\sum_{j=1}^N (RAA_j - \overline{RAA})^2}{N} \quad (21)$$

where N denotes $\#(RAA)$ within a match.

aja average. Denotes the average performance regarding *aja* of the current player among one match. The lower the feature is, the smaller angle and the less effort the player fires for and puts into hitting their targets.

$$\mathbf{F}_{\text{aja-avg}}(\mathbf{i}) = \overline{AJA} = \frac{\sum_{j=1}^N AJA_j}{N} \quad (22)$$

where N denotes $\#(AJA)$ within a match.

aja variance. Denotes the degree of dispersion of *aja* distributions of the current player among one match.

$$\mathbf{F}_{\text{aja-var}}(\mathbf{i}) = \text{Var}(AJA) = \frac{\sum_{j=1}^N (AJA_j - \overline{AJA})^2}{N} \quad (23)$$

where N denotes $\#(AJA)$ within a match.

C.2 Firing features

Inertial shot [39] percentage (isp) *Inertial shot* denotes that after an elimination is conducted by a player, who may apply several extra firings due to the inertia. *isp* represents the ratio of the number of *Inertial shot* times to the number of eliminations. α is a threshold and set as 0.15 seconds in our case.

$$\mathbf{IS}(\mathbf{E}_{kill}^{i \rightarrow o^*}[k]) = \begin{cases} 1, & \exists \mathbf{E}_{fire}^i \in (\mathbf{t}(\mathbf{E}_{kill}^{i \rightarrow o^*}[k]), \mathbf{t}(\mathbf{E}_{kill}^{i \rightarrow o^*}[k]) + \alpha) \\ 0, & \text{otherwise} \end{cases} \quad (24)$$

$$\mathbf{F}_{\mathbf{isp}}(\mathbf{i}) = \frac{\sum_k \mathbf{IS}(\mathbf{E}_{kill}^{i \rightarrow o^*}[k])}{\sum_n \mathbf{E}_{kill}^{i \rightarrow o^*}[n]} \quad (25)$$

First hit percentage (fhp) Denote how accurate a player is while spotting an opponent and reacting to fire. Event *reload* represents the action of changing the magazine while the firing is performed and the bullet is consumed. *Fire Round* denotes the unit of the firing round. *fhp* refers to the ratio of the number of the first firing event equivalent to a damage event while spotting at least one opponent within a time threshold ϵ to the number of times that the aforementioned event occurs while disregarding the equivalency and within the same time threshold ϵ . In our case, ϵ is set as 5 seconds (*i.e.*, 640 ticks).

$$\mathbf{E}_{reload}^i = \Delta(\mathbf{mag}(i)) > 0 \wedge \mathbf{t}(\mathbf{E}_{fire}^i[k]) - \mathbf{t}(\mathbf{E}_{fire}^i[k+1]) > 0 \quad (26)$$

$$\mathbf{FR}[i] = \{\mathbf{E}_{fire}^i[i] \mid \exists \mathbf{E}_{reload}^i \vee \mathbf{t}(\mathbf{E}_{fire}^i[i][k+1]) - \mathbf{t}(\mathbf{E}_{fire}^i[i][k]) > \epsilon\} \quad (27)$$

$$\mathbf{F}_{\mathbf{fhp}}(\mathbf{i}) = \frac{\#\{\mathbf{FR}[i][0] \mid \forall \mathbf{FR}[i][0] = \mathbf{E}_{damage}^{i \rightarrow o^*}\}}{\#\{\mathbf{FR}[i][0]\}} \quad (28)$$

Precision (precis) Denote the performance of firing accuracy. *precis* refers to the ratio of the number of damage caused by weapons to the total number of fires applied.

$$\mathbf{F}_{\mathbf{precis}}(\mathbf{i}) = \frac{\sum_k \mathbf{E}_{damage}^{i \rightarrow o^*}[k]}{\sum_n \mathbf{E}_{fire}^i[n]} \quad (29)$$

Strafing hit percentage (shp) Denote fire accuracy while *strafing*. *Strafe* allows a player to keep the view focused on an opponent while moving in a different direction. *shp* refers to the ratio of the number of damage caused while strafing to the number of damage caused.

$$\mathbf{F}_{\mathbf{shp}}(\mathbf{i}) = \frac{\sum_k \mathbf{E}_{damage \wedge strafe}^{i \rightarrow o^*}[k]}{\sum_n \mathbf{E}_{damage}^{i \rightarrow o^*}[n]} \quad (30)$$

Hit-group distribution (hgd) variance *Hit group* represents the body part that suffers damage, typically hit groups can be categorized as follows: *chest*, *generic*, *head*, *neck*, *left arm*, *right arm*, *left leg*, *right leg*, and *stomach*. *hgd* variance denotes the degree of dispersion of *hit group* distributions for the current player among one match.

$$HG_j = \sum_k \mathbf{E}_{damage \wedge hg(j)}^{i \rightarrow o^*}[k] \quad (31)$$

$$\overline{HG} = \frac{\sum_{j=chest}^{stomach} HG_j}{\sum_k \mathbf{E}_{damage}^{i \rightarrow o^*}[k]} \quad (32)$$

$$\mathbf{F}_{\mathbf{hgd}}(\mathbf{i}) = \text{Var}(HG) = \frac{\sum_{j=chest}^{stomach} (HG_j - \overline{HG})^2}{\sum_n \mathbf{E}_{damage}^{i \rightarrow o^*}[n]} \quad (33)$$

where $j \in \{\text{chest}, \text{generic}, \text{head}, \text{neck}, \text{left arm}, \text{right arm}, \text{left leg}, \text{right leg}, \text{stomach}\}$

Special hit Ratio (shr) *Special hit* denotes hit with sniper between 50 and 150 meters (*SH50-150*), head shot with sniper between 40 and 170 meters (*SHS40-170*), hit with normal weapon farther than 800 meters (*NH800+*) and headshot with normal weapon farther than 700 meters (*NHS700+*). In FPS games, hitting processes include using different weapons and shooting from different distances. In our game environment, the aforementioned four types of hits are considered to be potentially cheating combinations. *shr* denotes the ratio of the sum of the number of the aforementioned four types of *special hit* to the number of hits in one match.

$$\mathbf{SH}_{50-150}(\mathbf{i}) = \sum_k \mathbf{E}_{damage \wedge sniper \wedge (50 \leq dist(i,o) \leq 150)}^{i \rightarrow o^*}[k] \quad (34)$$

$$\mathbf{SHS}_{40-170}(\mathbf{i}) = \sum_k \mathbf{E}_{headshot \wedge sniper \wedge (40 \leq dist(i,o) \leq 170)}^{i \rightarrow o^*}[k] \quad (35)$$

$$\mathbf{NH}_{800+}(\mathbf{i}) = \sum_k \mathbf{E}_{damage \wedge normal \wedge (dist(i,o) \geq 800)}^{i \rightarrow o^*}[k] \quad (36)$$

$$\mathbf{NHS}_{700+}(\mathbf{i}) = \sum_k \mathbf{E}_{headshot \wedge normal \wedge (dist(i,o) \geq 700)}^{i \rightarrow o^*}[k] \quad (37)$$

$$\mathbf{F}_{\mathbf{shr}}(\mathbf{i}) = \frac{\mathbf{SH}_{50-150}(\mathbf{i}) + \mathbf{SHS}_{40-170}(\mathbf{i}) + \mathbf{NH}_{800+}(\mathbf{i}) + \mathbf{NHS}_{700+}(\mathbf{i})}{\sum_k \mathbf{E}_{damage}^{i \rightarrow o^*}[k]} \quad (38)$$

C.3 Elimination features

Time to kill (ttk) Denote the duration from the moment of the first damage caused to an opponent to the moment of the elimination of the opponent. In order to control the *ttk* to be each time one player attacks one enemy, the threshold of one statistical period of *ttk* is set to be 10 seconds. For instance, if

the attacking period time is over 10 seconds without killing the victims, this action time will not be recorded as *ttk*.

$$\mathbf{F}_{\text{ttk}}(\mathbf{i}) = \text{ELAPSE}(\mathbf{E}_{\text{damage}}^{i \rightarrow o}[0], \mathbf{E}_{\text{kill}}^{i \rightarrow o}) \quad (39)$$

ttk average. Denotes the average time regarding *ttk* of the current player among one match. The lower this feature is, the shorter the time the player kills victims.

$$\mathbf{F}_{\text{ttk-avg}}(\mathbf{i}) = \overline{TTK} = \frac{\sum_{j=1}^N TTK_j}{N} \quad (40)$$

where N denotes $\#(TTK)$ within a match.

ttk variance. Denotes the degree of dispersion of *ttk* distributions of the current player among one match.

$$\mathbf{F}_{\text{ttk-var}}(\mathbf{i}) = \text{Var}(TTK) = \frac{\sum_{j=1}^N (TTK_j - \overline{TTK})^2}{N} \quad (41)$$

where N denotes $\#(TTK)$ within a match.

First-blood percentage (fbp) *first-blood* denotes the very first elimination in one round. *fbp* denotes the ratio of the number of *first-blood* to the number of rounds in one match.

$$\mathbf{F}_{\text{fbp}}(\mathbf{i}) = \frac{\#(\mathbf{FK}(i))}{\#(\text{round})} \quad (42)$$

Onetap percentage (otp) *Onetap* denotes a head-shot fire event on an opponent that results in elimination without the use of sniper rifles, and where the inflicted damage is equal to or greater than 100 (the full health of a player). The *otp* represents the ratio of the number of *Onetap* instances to the number of times damage is inflicted by normal weapons.

$$\mathbf{ONETAP}(\mathbf{E}_{\text{kill}}^{i \rightarrow o^*}[k]) = \begin{cases} 1, & (\mathbf{E}_{\text{fire}}^i = \mathbf{E}_{\text{kill}}^{i \rightarrow o^*}[k]) \wedge (\mathbf{E}_{\text{damage}}^{i \rightarrow o^*} \geq 100) \\ 0, & \text{otherwise} \end{cases} \quad (43)$$

$$\mathbf{F}_{\text{otp}}(\mathbf{i}) = \frac{\sum_k \mathbf{ONETAP}(E_{\text{kill}}^{i \rightarrow o^*}[k])}{\sum_n \mathbf{E}_{\text{damage} \wedge \text{wp}(i) \neq \text{sniper rifle}}^{i \rightarrow o^*}[n]} \quad (44)$$

Occluder-penetration index (opi) *Occluder-penetration* denotes the elimination event that happens when the victim is eliminated behind one layer or more layers of occluders by a penetrated bullet. The occluders are typically walls, players (namely wall bang), or smoke. *opi* refers to a weighted index that reflects the extent of the average occluder-penetration eliminations conducted by the player. The use of the number of rounds within the division aims to eliminate bias brought

by that. In our case, the weights in α_i are 0.5, 1, 2, 0.5 respectively.

$$\mathbf{F}_{\text{opi}}(\mathbf{i}) = \frac{\mathbf{W}_i \alpha_i}{\#(\text{round})} \quad (45)$$

$$\text{where } \alpha_i = \begin{bmatrix} w_1 \\ w_2 \\ w_3 \\ w_4 \end{bmatrix},$$

$$\mathbf{W}_i = \begin{bmatrix} \sum_k \mathbf{E}_{\text{kill} \wedge p(1)}^{i \rightarrow o^*}[k] & \sum_n \mathbf{E}_{\text{kill} \wedge p(2)}^{i \rightarrow o^*}[n] & \sum_m \mathbf{E}_{\text{kill} \wedge p(2)}^{i \rightarrow o^*}[m] & \sum_j \mathbf{E}_{\text{kill} \wedge \text{ts}}^{i \rightarrow o^*}[j] \end{bmatrix}$$

Blind kill percentage (b kp) Denote the percentage of a player performing elimination while blinded. *b kp* refers to the ratio of the sum of elimination events where the attackers suffer a blinded effect to the number of eliminations.

$$\mathbf{F}_{\text{b kp}}(\mathbf{i}) = \frac{\sum_k \mathbf{E}_{\text{kill} \wedge \text{blind}}^{i \rightarrow o^*}[k]}{\sum_n \mathbf{E}_{\text{kill}}^{i \rightarrow o^*}[n]} \quad (46)$$

Critical hit percentage (chp) Denote the *critical hit* rate. *Critical hit* represents a successful damage event that applies to a particular hit group (typically, head) that deals more damage than a normal blow. *chp* refers to the ratio of the number of critical hits to the number of damage caused.

$$\mathbf{F}_{\text{chp}}(\mathbf{i}) = \frac{\sum_k \mathbf{E}_{\text{headshot}}^{i \rightarrow o^*}[k]}{\sum_n \mathbf{E}_{\text{damage}}^i[n]} \quad (47)$$

Average kill per round (akpr) Denote the average number of eliminations per round by a player in a match.

$$\mathbf{F}_{\text{akpr}}(\mathbf{i}) = \frac{\sum_k \mathbf{E}_{\text{kill}}^{i \rightarrow o^*}[k]}{\#(\text{round})} \quad (48)$$

C.4 Props utilization features

Flash efficiency index (fei) Denote how well a player utilizes the flash grenade. *fei* refers to the ratio of the total affection duration on the opponents minus that on the friendlies to the total affection duration.

$$\mathbf{F}_{\text{fei}}(\mathbf{i}) = \frac{\sum_k \text{ELAPSE}(\mathbf{E}_{\text{blind}}^{i \rightarrow o^*}[k]) - \sum_m \text{ELAPSE}(\mathbf{E}_{\text{blind}}^{i \rightarrow o^*}[m])}{\sum_n \text{ELAPSE}(\mathbf{E}_{\text{blind}}^{i \rightarrow o^*}[n])} \quad (49)$$

Props utilization index (pui) Denote how frequently a player utilizes props such as a high-explosive grenade, Molotov or incendiary, smoke grenade, or flash grenade. *pui* refers to the ratio of the sum of a player and the number of times different grenades are used to a fixed constant which reflects the maximum number of grenades used within this match for all players. ρ denotes the maximum number of props a player is allowed to carry per round. In our case, ρ is 5.

$$\mathbf{F}_{\text{pui}}(\mathbf{i}) = \frac{\#(\text{HEG}(i)) + \#(\text{INC}(i)) + \#(\text{SMK}(i)) + \#(\text{FLS}(i))}{\#(\text{player}) \times \#(\text{round}) \times \rho} \quad (50)$$

D Sense and Performance Features Classification

All features presented in this section are recombinations of features from the first two subsystems, categorized into two main types, i.e., sense features and performance features. For a detailed description of each feature, please refer to [Appendix B](#) and [Appendix C](#). The following merely enumerates the specific categorizations of the features and some brief descriptions.

D.1 Sense Features

Sense features indicate a player's in-game cognition, emphasizing their strategic acumen and tactical foresight.

- **Temporal Sense Features:**

- **Economy features:** Financial transactions and asset management, mirroring strategic resource allocation.
- **Movement features:** Spatial patterns, positioning, and navigation dynamics, indicating tactical awareness.
- **Flash features:** Strategic deployment of flash grenades during in-game engagements.
- **Grenade features:** Utilization of assorted grenades, highlighting understanding of map control.

- **Structured Sense Features:**

- **Flash efficiency index (fei):** Metrics gauging flash grenade efficiency.
- **Occluder-penetration index (opi):** Achieve eliminations at specific locations, demonstrating proficiency with the map.
- **Inertial shot percentage (isp):** As a normal human being's habitual firing after destroying an opponent.
- **Blind kill percentage (b kp):** Eliminations executed under visual impairment.
- **Props utilization index (pui):** Metrics showcasing prop usage across the whole match.

D.2 Performance Features

Performance features encapsulate a player's in-game efficacy, concentrating on engagement aptitude, aiming precision, and mechanism mastery.

- **Temporal Performance Features:**

- **Elimination Features:** Efficiency of eliminations and some special, difficult eliminations.
- **Weapon Fire Features:** Proficiency metrics across weapon categories, illuminating combat adeptness.
- **Damage Features:** The player's performance with respect to inflicting effective damage in-game.

- **Structured Performance Features:** The remaining structured features in [Appendix C](#).

E PCA on Structured Features

In [Section 4.2.1](#), we have demonstrated the distribution distinction between cheaters and normal players. In the following section, we will demonstrate the PCA visualization on the structured features to display their orthogonality on both *Aimbot* and *Wallhack* datasets. [Figure 13](#) illustrates the structured features PCA results for both datasets regarding the cheaters and normal players respectively. Horizontal and vertical axes represent the first principal component (PC1) and the second principal component (PC2), respectively. These principal components capture the directions of maximum variance in the data, showing where the data varies most. The unit circle in a correlation circle plot is a circle with a radius of 1, serving as a reference. Within this circle, the vectors (represented as arrows) demonstrate the magnitude and direction of the original variables' associations with the principal components. The arrow represents feature vectors, where the direction and length of each arrow indicate the relationship of the original data features with the principal components. The direction of the arrow shows the correlation direction of the feature with the principal components. If two arrows are pointing in similar directions, it means their corresponding features exhibit similar patterns of variation in the dataset. Length indicates the impact or correlation strength of that feature on the corresponding principal component. Longer arrows suggest that the feature contributes more significantly to the variance captured by that principal component, and vice versa. It is noticeable that within the same plot, most of the features are distinct from others by obtaining different directions and lengths of the arrow. We can also observe that the direction and length of the arrows across *Aimbot* and *Wallhack* datasets are distinctive, indicating that the data distributions of the corresponding features are statistically different. Additionally, there are differences in the direction and length of the arrows between cheaters and normal players within the same or across different datasets. Above all, the original features can not be replaced by PCA.

F Evaluation Metrics

The following are the detailed evaluation matrices that are used in [Section 6.3](#).

True Positives (TP), shown in [Equation 51](#), represents instances where the model accurately predicts the occurrence of cheating behavior.

$$TP = \sum_{i=1}^n I(y_i = 1 \wedge \hat{y}_i = 1) \quad (51)$$

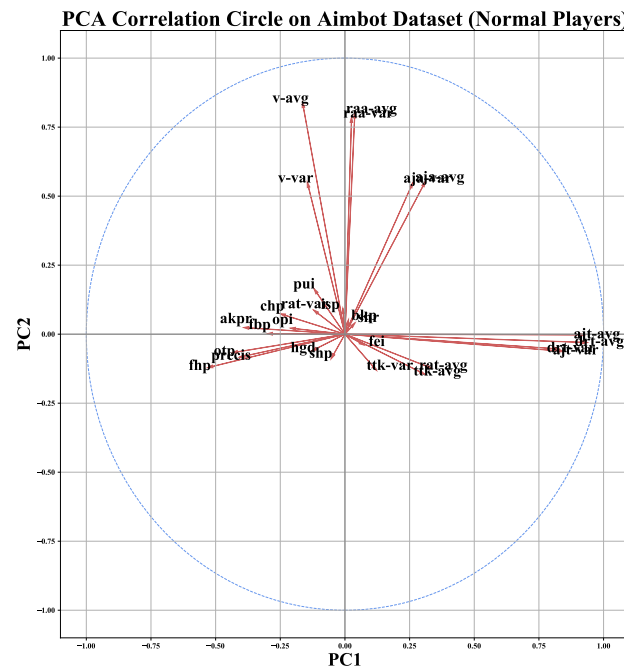
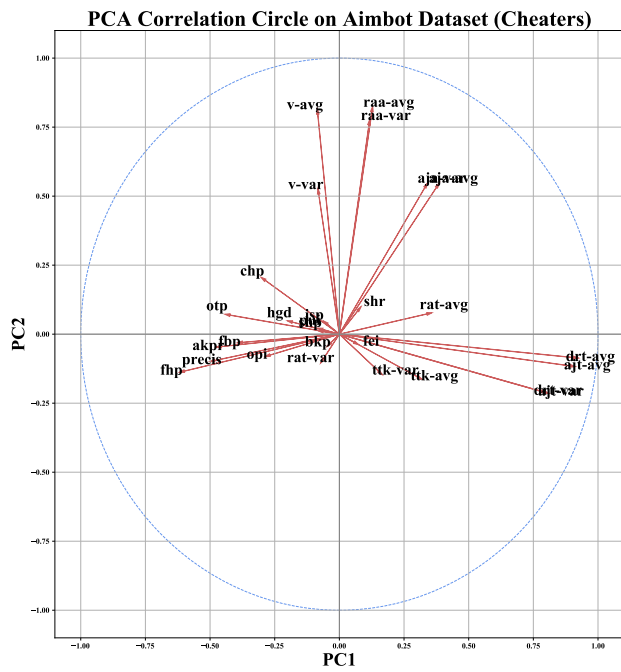
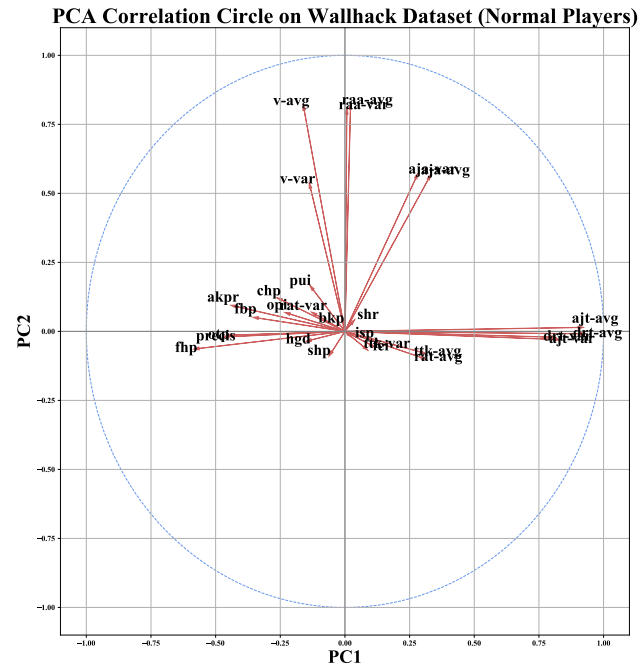
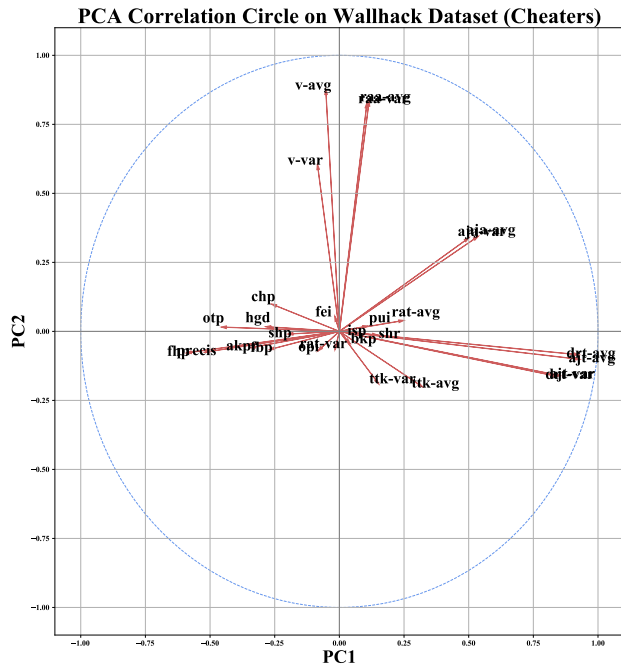


Figure 13: Structured Features PCA results on both datasets.

True Negatives (TN), represented in [Equation 52](#), denotes instances where the model correctly identifies the absence of cheating behavior.

$$TN = \sum_{i=1}^n I(y_i = 0 \wedge \hat{y}_i = 0) \quad (52)$$

False Positives (FP), represented in [Equation 53](#), encompass instances where the model erroneously predicts the presence of cheating behavior.

$$FP = \sum_{i=1}^n I(y_i = 0 \wedge \hat{y}_i = 1) \quad (53)$$

False Negatives (FN), represented in [Equation 54](#), are instances where the model inaccurately predicts the absence of cheating behavior.

$$FN = \sum_{i=1}^n I(y_i = 1 \wedge \hat{y}_i = 0) \quad (54)$$

In these equations, y_i denotes the true label, \hat{y}_i signifies the predicted label, and $I(\cdot)$ represents the indicator function.

Recall, represented in [Equation 55](#), measures the proportion of actual positive instances that were correctly identified by the model.

$$Recall = \frac{TP}{TP + FN} \quad (55)$$

Accuracy, as shown in [Equation 56](#), gives a holistic measure of the model's performance across both positive and negative classes.

$$Accuracy = \frac{TP + TN}{TP + TN + FP + FN} \quad (56)$$

AUC-ROC, denoted in [Equation 57](#), is the area under the receiver operating characteristic curve, indicating the model's capability to differentiate between positive and negative classes. It is computed by integrating the ROC curve, as shown below, where TPR (True Positive Rate) is synonymous with Recall, and FPR (False Positive Rate) is defined as $\frac{FP}{TP + FN}$.

$$AUC - ROC = \int_0^1 TPR(FPR) dFPR \quad (57)$$

NPV, shown in [Equation 58](#), is the proportion of actual negative instances among all instances predicted as negative.

$$NPV = \frac{TN}{TN + FN} \quad (58)$$